4. A ressonância 1/1 com Júpiter

4.1. Introdução

A ressonância 1/1 com Júpiter ocorre numa faixa de aproximadamente 0.4 UA de largura, centrada em 5.2 UA. Ela é caracterizada por um regime de órbitas girino ao redor dos pontos Lagrangeanos L_4 e L_5 de Júpiter, tal que o ângulo ressonante $\sigma_{1/1} = \lambda - \lambda_J$ libra em torno de $\pm 60°$, respectivamente. Associada a esta ressonância existe uma população de mais de 600 asteróides que recebe o nome de Troianos, sendo que cerca de 60% deles orbita em torno de L_4, enquanto que 40% o faz em torno de L_5.

A estabilidade a longo prazo dos Troianos tem sido estudada por Levison, Shoemaker e Shoemaker (1997), que mostraram que estes asteróides são estáveis ao longo da idade do Sistema Solar. Os Troianos seriam objetos primordiais na ressonância 1/1, provavelmente capturados ainda durante as etapas finais da formação do Júpiter (Marzari e Scholl 1998). Simulações numéricas também mostram que estes asteróides teriam sofrido uma evolução colisional importante (Marzari et al. 1997), que deveria se manifestar na existência de famílias (Milani 1993).

Neste capítulo apresentamos os resultados de dois trabalhos sobre a dinâmica dos Troianos. No primeiro desenvolvemos um modelo semi-analítico para o estudo da dinâmica a longo prazo da ressonância 1/1. A seguir, este modelo é aplicado para determinar elementos próprios dos Troianos reais e procurar por famílias de asteróides, que permitiriam, eventualmente, reconstruir a história colisional destes objetos. No segundo trabalho, a dinâmica da ressonância 1/1 é discutida no âmbito da migração

planetária, analisando como este fenômeno pode afetar a estabilidade dos Troianos reais, e como isto pode ser utilizado para colocar limites à própria migração.

4.2. O modelo semi-analítico

Nosso modelo semi-analítico para descrever a dinâmica a longo prazo dos asteróides Troianos baseia-se em três aproximações: (i) a utilização de variáveis locais, que permitem transformar a libração do ângulo ressonante $\sigma_{1/1}$ numa circulação, facilitando assim a aplicação de um método perturbativo clássico (método de Hori (Hori 1966)); (ii) a construção de um desenvolvimento assimétrico da função perturbadora para representar o movimento das órbitas girino na ressonância 1/1; (iii) a combinação do método perturbativo com a teoria dos invariantes adiabáticos, utilizando o fato de que os diferentes graus de liberdade do problema estão bem separados no espaço das freqüências próprias. A seguir, analisamos com mais detalhe cada uma delas.

4.2.1. Variáveis locais

O principal problema no tratamento de problemas ressonantes através de métodos perturbativos é que o ângulo ressonante (no caso $\sigma_{1/1}$) possui uma freqüência própria muito próxima de zero. Isto faz aparecer os pequenos divisores na solução por série do problema, o que torna o método perturbativo não-convergente. Para evitar este problema, é necessário então transformar o ângulo ressonante num novo ângulo cuja freqüência seja diferente de zero. A modo de exemplo, vamos considerar o problema de três corpos restrito elíptico planar médio. O problema tem dois graus de liberdade e, no tratamento perturbativo usual, a Hamiltoniana é separada na forma

$$H(J_1, J_2, \theta_1, \theta_2) = H_0(J_1, J_2, \theta_1) + \varepsilon H_1(J_1, J_2, \theta_1, \theta_2) \tag{4.1}$$

sendo $\varepsilon \ll 1$ um pequeno parâmetro que depende da excentricidade do corpo perturbador, e J_i, θ_i variáveis conjugadas. Em outras palavras, H_0 corresponde à parte circular do problema e H_1 à parte elíptica. A Hamiltoniana H_0 possui um grau de liberdade, portanto é integrável. Ela define a topologia básica da ressonância, onde θ_1 é um ângulo que libra. Assim, dadas condições iniciais J_1^0, J_2^0, θ_1^0, procede-se a achar as variáveis ação e ângulo $\overline{J}_1, \overline{\theta}_1, \overline{J}_2 = J_2^0$ de H_0, de forma que agora $\overline{\theta}_1$ é um ângulo que

circula com freqüência constante diferente de zero. Estas variáveis são logo introduzidas em H_1, fazendo-se a seguir uma média sobre $\overline{\theta}_1$, de forma a eliminar um grau de liberdade e ficar com uma Hamiltoniana $\overline{H}(\overline{J}_1, \overline{J}_2, \overline{\theta}_2)$ que é integrável (Henrard 1990).

A desvantagem deste método está no fato de ter que determinar as variáveis ação e ângulo de H_0 para cada condição inicial, o que consome muito tempo de cálculo. Além disso, na passagem $\theta_1 \to \overline{\theta}_1$ perde-se qualquer informação sobre a fase de θ_1, o que introduz complicações na hora de inverter a solução para obter $J_1(t), \theta_1(t)$. Em nosso trabalho, apresentamos uma aproximação diferente ao problema, onde estes inconvenientes são resolvidos substituindo o cálculo de variáveis ação e ângulo pela transformação a variáveis locais, como explicamos a seguir.

A dinâmica de H_0 é caraterizada pela libração de θ_1 em torno de θ_c. Mais precisamente, introduzindo as variáveis $k_1 + ih_1 = \sqrt{2J_1}\exp(i\theta_1)$, a libração acontece em torno do ponto $k_c + ih_c$. Assim, a idéia por trás da transformação a variáveis locais consiste em fazer uma transferência:

$$\overline{k}_1 + i\overline{h}_1 = (k_1 - k_c) + i(h_1 - h_c) \tag{4.2}$$

de forma que o novo ângulo $\overline{\theta}_1$ não mais libra em torno de θ_c, mas circula em torno de $(\overline{k}_c, \overline{h}_c) = (0, 0)$. Isto é feito mediante uma transformação canônica, que gera uma nova Hamiltoniana $\overline{H}(\overline{J}_1, \overline{J}_2, \overline{\theta}_1, \overline{\theta}_2)$, onde os ângulos $\overline{\theta}_1, \overline{\theta}_2$ circulam e têm freqüências próprias diferentes de zero. Portanto, o problema dos pequenos divisores nas séries perturbativas desaparece. A vantagem da transformação (4.2) é que é muito mais simples e transparente que o cálculo de variáveis ação ângulo e, além disso, só requer que se determinem os valores J_c, θ_c do centro de libração, que não são outra coisa que os pontos de equilíbrio da Hamiltoniana H_0.

4.2.2. Desenvolvimento assimétrico

Uma vez introduzidas as variáveis locais, o passo seguinte para a construção do nosso modelo é achar uma expressão analítica para a Hamiltoniana H, que possa ser manipulada algebricamente. Na maioria dos estudos analíticos sobre a ressonância 1/1, utilizam-se expansões em coordenadas Cartesianas que não resultam adequadas para a determinação de elementos próprios. Além disso, os desenvolvimentos clássicos em variáveis ângulo momento, do tipo Laplaciano, não são convergentes no caso da res-

sonância 1/1.

Para evitar estes inconvenientes, em nosso modelo desenvolvemos uma expansão em série de Taylor-Fourier da Hamiltoniana, baseada no desenvolvimento assimétrico da função perturbadora (Ferraz-Mello e Sato 1989). A idéia deste desenvolvimento é que o movimento de libração em torno do ponto k_c, h_c pode ser representado utilizando-se uma expansão da Hamiltoniana em série de Taylor em torno de k_c, h_c. Em nosso caso, a Hamiltoniana é expandida primeiro em série de Taylor nos momentos $\overline{J}_i$ e, posteriormente, os coeficientes desta expansão, que são funções periódicas dos ângulos $\overline{\theta}_i$, são expandidos em série de Fourier.

4.2.3. Invariância adiabática

A transformação para variáveis locais evita a ocorrência de pequenos divisores nas séries perturbativas. De fato, a Hamiltoniana (4.1) adota a forma

$$\overline{H}(\overline{J}_1, \overline{J}_2, \overline{\theta}_1, \overline{\theta}_2) = \overline{H}_0(\overline{J}_1, \overline{J}_2) + \mu \overline{H}_1(\overline{J}_1, \overline{J}_2, \overline{\theta}_1, \overline{\theta}_2) \tag{4.3}$$

onde $\mu \ll 1$, sendo possível achar uma aproximação integrável de $\overline{H}$ através do método clássico de Hori, onde a solução de $\overline{H}_0$ constitui o "kernel" do método. No entanto, no caso da ressonância 1/1 é possível tirar vantagem do fato que os graus de liberdade possuem períodos característicos bem diferentes, e utilizar a teoria dos Invariantes Adiabáticos para resolver a Hamiltoniana.

Sejam ν_1, ν_2 as freqüências características de $\overline{\theta}_1, \overline{\theta}_2$, respectivamente. Assumindo que $\epsilon = \nu_2/\nu_1 \ll 1$, é possível fixar $\overline{J}_2, \overline{\theta}_2$ e resolver a Hamiltoniana $\overline{H}$ como se fosse um sistema de só um grau de liberdade, $\overline{J}_1, \overline{\theta}_1$. Aplicando o método de Hori a este sistema, acham-se novas variáveis $\overline{J}_1^*, \overline{\theta}_1^*, \overline{J}_2^*, \overline{\theta}_2^*$, tais que a nova Hamiltoniana é $\overline{H}^*(\overline{J}_1^*, \overline{J}_2^*, \overline{\theta}_2^*)$, e pode ser resolvida como se fosse um sistema de só um grau de liberdade. O momento $\overline{J}_1^*$ é uma constante até ordem ϵ, e recebe o nome de invariante adiabático. Mas de fato, $\overline{J}_1^*$ depende de $\overline{J}_2^*, \overline{\theta}_2^*$ através de termos da ordem de ϵ^2. Como estes termos são periódicos, podem ser eliminados fazendo-se uma média sobre o período de $\overline{\theta}_2^*$, obtendo-se um valor de $\overline{J}_1^*$ que pode ser considerado como o elemento próprio associado ao primeiro grau de liberdade. Finalmente, a solução de $\overline{H}^*$ fornece o elemento próprio associado ao segundo grau de liberdade.

Este formalismo pode ser estendido a qualquer sistema com N graus de liberade

tais que $\nu_N \ll \ldots \ll \nu_2 \ll \nu_1$. É o caso dos Troianos de Júpiter, onde o período de $\sigma_{1/1}$ é da ordem de 150 anos, o período de ϖ é da ordem 3500 anos, e o período de Ω é da ordem de 10^5 anos. A vantagem deste formalismo com relação à Eq. (4.3) é que o "kernel" do método de Hori é mais completo do que H_0, já que contém embutido termos da ordem de μ, que na Eq. (4.3) só aparecem em H_1.

Nosso modelo inclui as principais perturbações devidas à variação secular da órbita de Júpiter, assim como os termos associados às perturbações diretas dos outros planetas Jovianos. Isto poderia gerar a aparição de ressonâncias seculares entre os graus de liberdade do problema, o que invalidaria a aproximação adiabática da solução. Porém, sabemos a partir de outros estudos (Morais 2001) que a única ressonância secular que acontece na ressonância 1/1 é a ν_{16}, envolvendo o nodo do asteróide e de Júpiter. Esta ressonância manifesta-se nas grandes amplitudes de libração, onde quase nenhum Troiano real é observado.

4.3. Elementos próprios e famílias

Usando o nosso modelo semi-analítico, determinamos os elementos próprios de 514 Troianos de Júpiter, incluindo os objetos numerados e multioposicionais conhecidos em dezembro de 2000. A precisão destes elementos próprios sobre 50 milhões de anos é da ordem de 0.1% (r.m.s.), o que representa um erro aproximadamente duas vezes maior que o obtido a partir de estudos puramente numéricos (Bien e Schubart 1987; Milani 1993).

Com estes elementos próprios, identificamos as famílias de asteróides, através do método de Aglomeração Hierárquica (Zappalà et al. 1990). Achamos cinco famílias em torno de L_4 e apenas duas famílias em torno de L_5. As mais relevantes são as famílias de 1647 Menelaus e 2148 Epeios, ambas em torno de L_4, contando 24 e 19 membros respectivamente. Estas famílias seriam o resultado da evolução colisional dos Troianos de L_4 ao longo da idade do Sistema Solar. No entanto, não foi possível detectar aglomerações similares em torno de L_5. Para explicar isto, uma alternativa seria, simplesmente, que cada grupo teve uma história colisional diferente. Mas a ausência de famílias em L_5 também poderia ser conseqüência de eventuais diferenças na estabilidade a longo prazo de cada ponto Lagrangeano. De fato, estas diferenças existem no âmbito da dinâmica não-conservativa (Murray 1994; Gomes 1998), e poderiam contribuir para

evaporar as famílias formadas em L_5, mais rapidamente do que as formadas em L_4. A diferença no número de famílias entre L_4 e L_5 poderia estar vinculada ao fato da população observada de L_4 ser maior do que a de L_5, o que constitui um problema ainda em aberto.

4.4. Migração planetária e estabilidade dos Troianos

Para encerrar nosso estudo da ressonância 1/1, fazemos uma análise da estabilidade desta ressonância sob o efeito da migração planetária. A idéia por trás deste estudo é que, como conseqüência da migração, os planetas teriam atravesado no pasado por várias ressonâncias mútuas de movimentos médios. A passagem por estas ressonâncias, ou a eventual captura temporária nas mesmas, fez os planetas evoluir temporariamente em órbitas caóticas, pudendo gerar instabilidades significativas nos asteróides Troianos. A pergunta é: quão significativas?

Para responder a isto fazemos uma série de simulações numéricas onde Júpiter e Saturno são colocados "ad hoc" em diferentes ressonâncias mútuas, estudando como isto afeta a evolução dinâmica de partículas de teste na ressonância 1/1 com Júpiter. É importante destacar que nós não simulamos a migração dos planetas, mas apenas colocamos eles nas possíveis ressonâncias. Além disso, mesmo quando as simulações levam em conta as perturbações dos quatro planetas Jovianos, só Júpiter e Saturno são colocados em ressonância mútua. Finalmente, devemos levar em conta que os nossos resultados são interpretados assumindo a hipótese de que os Troianos já existiam quando a migração ocorreu.

Nas nossas simulações estudamos três ressonâncias: 2/1, 7/3 e 5/2. De acordo com os modelos clássicos de migração (Fernández e Ip 1984; Hahn e Malhotra 1999), estas ressonâncias poderiam ter sido atravesadas pelo sistema Júpiter-Saturno. Nossos resultados mostram que, com os planetas na ressonância 2/1, quase 90% das mais de 1500 partículas de teste inicialmente na região dos Troianos escapam em menos de 5000 anos. Com os planetas na ressonância 5/2, a região dos Troianos é esvaziada quase totalmente em aproximadamente 10^6 anos. Finalmente, com os planetas na ressonância 7/3, a depleção é bem mais fraca, e quase 60% das partículas de teste iniciais sobrevivem na região dos Troianos ainda após 5 milhões de anos.

Nossa conclusão é que Júpiter e Satruno não teriam atravesado a ressonância 2/1

durante a migração. Porém, a existência dos Troianos de Júpiter é compatível com a eventual passagem dos planetas pela ressonância 7/3. Ainda mais, os Troianos poderiam sobreviver a uma eventual captura temporária dos planetas na ressonância 5/2.

Anexo:

A semianalytical model for the motion of the Trojan asteroids: Proper elements and families

Icarus **153**, 391–415 (2001)
doi:10.1006/icar.2001.6699, available online at http://www.idealibrary.com on IDEAL®

A Semianalytical Model for the Motion of the Trojan Asteroids: Proper Elements and Families

C. Beaugé[1]

Observatorio Astronómico, Universidad Nacional de Córdoba, Laprida 854, 5000 Córdoba, Argentina

and

F. Roig

Instituto Astronômico e Geofísico, Universidade de São Paulo, Avenida Miguel Stefano 4200, 04301-904 São Paulo, SP, Brazil

Received January 29, 2001; revised June 21, 2001

In this paper we develop a semianalytical model to describe the long-term motion of Trojan asteroids located in tadpole orbits around the L_4 and L_5 jovian Lagrangian points. The dynamical model is based on the spatial elliptic three-body problem, including the main secular variations of Jupiter's orbit and the direct perturbations of the remaining outer planets. Based on ideas introduced by A. H. Jupp (1969, *Astron. J.* 74, 35–43), we develop a canonical transformation which allows the transformation of the tadpole librating orbits into circulating orbits. The disturbing function is then explicitly expanded around each libration point by means of a Taylor–Fourier asymmetric expansion.

Making use of the property in which the different degrees of freedom in the Trojan problem are well separated with regard to their periods of oscillation, we are able to find approximate action-angle variables combining Hori's method with the theory of adiabatic invariants. This procedure is applied to estimate proper elements for the sample of 533 Trojans with well determined orbits at December 2000. The errors of our semianalytical estimates are about 2–3 times larger than those previously obtained with numerical approaches by other authors.

Finally, we use these results to search for asteroidal families among the Trojan swarms. We are able to identify and confirm the existence of most of the families previously detected by Milani (1993, *Celest. Mech. Dynam. Astron.* 57, 59–94). The families of *Menelaus* and *Epeios*, both around L_4, are the most robust candidates to be the by-product of catastrophic disruption of larger asteroids. On the other hand, no significant family is detected around L_5.

Key Words: **asteroids, dynamics; asteroids, Trojans; celestial mechanics; resonances.**

1. INTRODUCTION

The Trojans (or Jupiter Trojans) are a group of asteroids located in the vicinity of Jupiter's orbit when observed in the semimajor axis domain. Their orbits are characterized by an oscillation of the angle $\lambda - \lambda_1$ around one of the equilateral Lagrangian points L_4, L_5 (λ and λ_1 are the mean longitudes of the asteroid and Jupiter, respectively). These orbits are usually referred to as "tadpole" orbits due to the shape of the zero-velocity curves of the three-body problem in the synodic reference frame. The Trojan swarms can be further divided into two groups: the Greeks, orbiting the L_4 point, and the genuine Trojans, orbiting L_5.

Even though theoretical studies of equilateral equilibrium configurations of the three-body problem date back to Lagrange in the late eighteenth century, the first asteroid in such a location was observed only in 1906. It was later designated as (*588*) *Achilles* and was found orbiting L_4. The same year a second body, (*617*) *Patroclus*, was found in L_5. Since then, an ever increasing number of asteroids have been discovered. The present number of Trojans (as of December 2000) with well determined orbits contained in the Asteroids Database of Lowell Observatory (`ftp.lowell.edu/pub/elgb/astorb.dat`) amounts to 533. If we include the bodies with poorly determined orbits, this number grows to more than 800. Even this number may be only the tip of the iceberg. Levison *et al*. (1997) predict that as many as two million asteroids (with size larger than one kilometer) may in fact lie around these points, thus rivaling the population found in the main belt.

The basic idea of the present study is to develop a semianalytical model for the dynamics in the 1 : 1 mean motion resonance. We focus on the long-term behavior of bodies in tadpole orbits in the vicinity of the equilateral Lagrangian points, and we present some results concerning the long-term dynamical evolution of these asteroids. Our aim is to construct a model that can be applied to a qualitative study of the resonant structure in the

[1] Present address: Instituto Nacional de Pesquisas Espaciais, Avenida dos Astronautas 1758, (12227-010) São José dos Campos, SP, Brazil.

0019-1035/01 $35.00

tadpole regime (e.g., secular resonances inside the libration zone of each Lagrange point), but the main goal of the present paper is the determination of proper elements for all known Trojans. Although we center our study on Jupiter Trojans, it is worth noting that the scope of this work is not restricted to this subsystem. Specifically, one of the main advantages of analytical studies is the universality of the model: It may be applied to the case of any other perturber.

We note that, up to now, all the determinations of Trojan proper elements have been carried out numerically. Perhaps the most complete study to date is due to Milani (1993). He performed a numerical integration over timescales of 10^6 yr, and applied a Fourier analysis to the output to determine the fundamental frequencies of the free oscillations and their amplitudes (i.e., synthetic theory). These latter constitute his proper elements. A similar approach was recently employed by Burger *et al.* (1998) and Pilat-Lohinger *et al*. (1999), although their study was more concerned with chaotic orbits. On the other hand, analytical and semianalytical approaches have only been made in the case of main belt asteroids (e.g., Williams 1969, Milani and Knežević 1990, 1994, Lemaítre and Morbidelli 1994, Knežević *et al*. 1995, Knežević and Milani 2001).

From a theoretical point of view, proper elements are integrals of motion of a given dynamical system. They are values of certain actions of the system that remain constant in time (see Lemaítre 1993 and Knežević 1994 for discussions). However, in practice almost all real dynamical systems are nonintegrable, so these integrals of motion do not really exist. In the best case we can find only quasi-integrals, which are only approximately constant in time, provided the chaos is sufficiently localized and slow so that the calculated proper elements still make sense and contain meaningful information about the dynamics. In some sense, studies of proper elements constitute a kind of "archaeology" of the Solar System. Within the present observed distribution of bodies we search for relics of their original dynamical structure: parameters that have remained almost unchanged for hundreds of millions of years. And it is through these relics that we hope to deepen our understanding of the origin of these bodies.

When determining proper elements for a given dynamical system, the main sources of approximation for the results are: (i) nonintegrability (chaos) of the system, which causes the real motion of the system to be nonquasiperiodic in nature; (ii) very long period perturbations, resulting from quasi-commensurabilites between the different frequencies of the system; and (iii) limitations of the dynamical model, which include approximations both in the analytical model and in the model of the Solar System. While the two latter approximations generate periodic variations of the calculated proper elements (thus influencing only their precision), the first one concerns their very existence and can make them meaningless.

The question that arises is: What is the magnitude of the chaos in the Trojan belt? Although this question has been addressed several times in past years, we still do not have a complete answer. Milani (1993), in his study of proper elements of Trojan asteroids, found several cases of what he refers to as "stable chaos," i.e., orbits with positive Lyapunov exponents (in some cases even quite large), but which do not exhibit any gross instability over very long timescales. Only very few asteroids were found with significant instabilities on timescales of the order of 10^6 yr, all of them lying in the vicinity of secular resonances of the node. Similar results were also found by Pilat-Lohinger *et al*. (1999) and by Marzari and Scholl (2000). Giorgilli and Skokos (1997) used Nekhoroshev theory to study the stability of the tadpole libration region in the Sun–Jupiter–asteroid model. Although they found a zone around the Lagrange points which is effectively stable over the age of the universe, this region is too small and only includes a few of the real Trojans. Most of the present Trojan population seems to lie outside this stable region, which implies that chaotic diffusion and global instability cannot be ruled out for these asteroids. A different type of study was undertaken by Levison *et al*. (1997). They performed numerical integrations of real and fictitious bodies over timescales of 10^9 yr and for various initial conditions. Although a number of particles showed lifetimes much shorter than the age of the Solar System, about 90% of the initial conditions compatible with the Trojan swarm survived the complete simulation, exhibiting (apparently) stable behavior. Thus, although at present we are not able to provide a precise quantification of the stability of the real Trojans, there is a certain confidence that whatever instability or chaotic diffusion exist must be extremely slow. For most of the Trojan population, the present dynamical behavior should remain essentially invariant for timescales of at least 10^8–10^9 yr. Over these timescales, proper elements are certainly meaningful and can be considered good indicators of the original dynamical structure.

The present paper is organized as follows: Section 2 presents an application of the method of adiabatic invariance to Hori's averaging method in canonical systems (Hori 1966). This is the approach that will be used to determine the solution of the sets of canonical transformations, eventually leading to the determination of the proper elements. In Section 3 we introduce the general semianalytic expansion of the Hamiltonian of the three-body problem in the vicinity of the 1 : 1 resonance. Section 4 discusses the hierarchical separation of the different degrees of freedom of the problem and their successive elimination. Determination of proper elements follows in Section 5, as well as their comparison with previous studies. Identification of possible asteroidal families is treated in Section 6. Finally, Section 7 is devoted to conclusions.

2. AVERAGING METHODS WITH ADIABATIC INVARIANCE

Many characteristics of the Trojan asteroids complicate the elaboration of an analytical model for their long-term motion. They have moderate-to-low eccentricities ($e \leq 0.2$), but they can reach very high inclinations (up to 40°) with respect to Jupiter's orbit. The resonant angle $\sigma = \lambda - \lambda_1$ may show large

amplitudes of libration: $D \leq 40^\circ$ (we define D as half the difference between the maximum and minimum values of σ, i.e., $D = (\sigma_{\max} - \sigma_{\min})/2$). Moreover, in several cases the longitude of perihelion ϖ can show what is usually referred to as "kinematic" or "paradoxal" libration. In other words, ϖ does not take all the values from zero to 2π, although from the topological point of view the motion is related to a circulation. Fortunately, there is one feature that counteracts these difficulties. It refers to the fact that the different degrees of freedom of the system are well separated with respect to their periods. In other words, while the period of libration associated with the resonant angle σ is typically about 150 yr, the period of oscillation of the longitude of perihelion ϖ is of the order of 3500 yr, while the period of the longitude of the ascending node is even longer: 10^5–10^6 yr. It is this property we exploit in the modeling of our problem.

In this section we concentrate on the development of a general procedure to analyze multidimensional Hamiltonian systems having this kind of "hierarchical" separation of the different degrees of freedom. In the next section the results obtained in this manner will be applied to the particular case of the Trojans.

2.1. *System with Two Degrees of Freedom*

We begin by supposing a generic two-degree-of-freedom system defined by a Hamiltonian function F,

$$F \equiv F(J, \theta) = F_0(J_1, J_2) + \mu F_1(J_1, J_2, \theta_1, \theta_2), \qquad (1)$$

where μ is a small parameter and (J, θ) are action-angle variables of F_0. We will assume that the unperturbed frequencies $\nu_i = \partial F_0/\partial J_i$ are finite and large, i.e., neither θ_1 nor θ_2 are resonant angles. Furthermore, we will suppose that there are no significant commensurabilities between these frequencies. In other words, there are no small integer values k, l such that $k\nu_1 + l\nu_2 \simeq 0$. Then, we can solve this system by using a classical averaging process such as Hori's method. We search for a generating function $B(J^*, \theta^*)$ of the transformation $(J, \theta) \rightarrow (J^*, \theta^*)$ to new canonical variables (J^*, θ^*) such that the transformed Hamiltonian is $F^* = F^*(J^*)$. In order to perform all calculations explicitly, imagine that we have F written as a *truncated* Fourier–Taylor series of the type

$$F(J, \theta) = \sum_{i,j,k,l} A_{i,j,k,l} (J_1)^i (J_2)^j E^{\sqrt{-1}(k\theta_1 + l\theta_2)}, \qquad (2)$$

where $E^x = \exp(x)$ and the coefficients $A_{i,j,k,l}$ (constant with respect to the variables) are, for the time being, undetermined. The transformation equations between both systems of variables, up to first order, are given by

$$\begin{aligned} J_1 &= J_1^* + \partial B_1/\partial \theta_1^* \\ \theta_1 &= \theta_1^* - \partial B_1/\partial J_1^* \\ J_2 &= J_2^* + \partial B_1/\partial \theta_2^* \\ \theta_2 &= \theta_2^* - \partial B_1/\partial J_2^*, \end{aligned} \qquad (3)$$

where the first-order generating function has the form

$$B_1 = -\sqrt{-1} \sum_{i,j} \sum_{k,l \neq 0} \frac{A_{i,j,k,l}}{k\nu_1^* + l\nu_2^*} (J_1^*)^i (J_2^*)^j E^{\sqrt{-1}(k\theta_1^* + l\theta_2^*)}, \qquad (4)$$

and the new Hamiltonian is $F^*(J_1^*, J_2^*) = F_0(J_1^*, J_2^*)$. The new frequencies ν_1^*, ν_2^* are given, in terms of the new actions, as

$$\begin{aligned} \nu_1^* &\equiv \frac{\partial F^*}{\partial J_1^*} = \sum_{i,j} i A_{i,j,0,0} (J_1^*)^{(i-1)} (J_2^*)^j \\ \nu_2^* &\equiv \frac{\partial F^*}{\partial J_2^*} = \sum_{i,j} j A_{i,j,0,0} (J_1^*)^i (J_2^*)^{(j-1)}. \end{aligned} \qquad (5)$$

It is worth noting that B_1 is a function of order $\mu \ll 1$, so the difference between (J, θ) and (J^*, θ^*) is also of order μ. Moreover, the difference between the old unperturbed frequencies ν_i and the new ones ν_i^* is of order μ, and whenever ν_1 and ν_2 are not commensurable, so should ν_1^* and ν_2^* be. In other words, we can assure that up to order μ there are no small integers k, l such that $k\nu_1^* + l\nu_2^* \simeq 0$. Then, the solution of system (3) can be found by an iterative procedure of successive approximations.

For the discussion that follows, it is important to mention that it is not necessary to restrict Hori's method to the first order in μ. Nevertheless, all the calculations are easier and the procedure developed in our model becomes much clearer.

2.2. *Hierarchical Structure and Adiabatic Invariance*

Let us concentrate on the solution of system (3) and the search for the new action-angle variables (J^*, θ^*). Let us forget, for the time being, that this system corresponds to a canonical transformation and think about it as a system of four algebraic equations corresponding to two different sets of variables (degrees of freedom). Knowing $(J_1, J_2, \theta_1, \theta_2)$, we wish to determine $(J_1^*, J_2^*, \theta_1^*, \theta_2^*)$ so as to satisfy (3). Instead of taking all equations simultaneously, we will divide the system into two parts, adopting a hypothesis of adiabatic invariance as follows. Let us suppose that the unperturbed frequencies of each degree of freedom satisfy the condition

$$\nu_1 \gg \nu_2, \qquad (6)$$

and let us introduce the small parameter $\epsilon = \nu_2/\nu_1$. We know, for example, that this kind of relation holds in the Trojan case. Since the first degree of freedom is much faster than the second, we can solve it separately, assuming fixed values for (J_2^*, θ_2^*), and writing the solution in terms of these values.

Let us rewrite the subsystem corresponding to the first degree of freedom explicitly as

$$J_1 = \bar{J}_1^* - \frac{\partial}{\partial \theta_1^*} \left(\sum_{i,j} \sum_{k,l \neq 0} \frac{\sqrt{-1} A_{i,j,k,l}}{k\bar{\nu}_1^* + l\nu_2^*} (\bar{J}_1^*)^i (J_2^*)^j E^{\sqrt{-1}(k\bar{\theta}_1^* + l\theta_2^*)} \right)$$

$$\theta_1 = \bar{\theta}_1^* + \frac{\partial}{\partial \bar{J}_1^*}\left(\sum_{i,j}\sum_{k,l\neq 0}\frac{\sqrt{-1}A_{i,j,k,l}}{k\bar{\nu}_1^* + l\nu_2^*}(\bar{J}_1^*)^i (J_2^*)^j E^{\sqrt{-1}(k\bar{\theta}_1^* + l\theta_2^*)}\right), \tag{7}$$

where we suppose (J_2^*, θ_2^*) to be fixed parameters (with respect to time). Since this is not true in the real system (3), we will designate the results obtained by this approximation as $(\bar{J}_1^*, \bar{\theta}_1^*)$. In other words, (J_1^*, θ_1^*) will be the real (averaged to the first order) action-angle variables, and $(\bar{J}_1^*, \bar{\theta}_1^*)$ will be the approximations obtained from (7). Solving this system by iterations, and denoting (J_1^0, θ_1^0) as the initial values at $t = 0$, we obtain

$$\begin{aligned} \bar{J}_1^* &= \bar{J}_1^*\big(J_1^0, \theta_1^0; J_2^*, \theta_2^*\big) \\ \bar{\theta}_1^* &= \bar{\theta}_1^*\big(J_1^0, \theta_1^0; J_2^*, \theta_2^*\big). \end{aligned} \tag{8}$$

Now, we need to relate $(\bar{J}_1^*, \bar{\theta}_1^*)$ to the original (J_1^*, θ_1^*). From the theory of adiabatic invariants (see Henrard, 1993) we know that the difference between the solution of the system where (J_2^*, θ_2^*) are fixed and the one where these quantities are slowly varying with time is of the order of ϵ, i.e.,

$$\begin{aligned} \bar{J}_1^* - J_1^* &\propto \epsilon\mathcal{K}(\bar{J}_1^*, \bar{\theta}_1^*; J_2^*, \theta_2^*) \\ \bar{\theta}_1^* - \theta_1^* &\propto \epsilon\mathcal{L}(\bar{J}_1^*, \bar{\theta}_1^*; J_2^*, \theta_2^*), \end{aligned} \tag{9}$$

where $\mathcal{K}$ and $\mathcal{L}$ are functions of order unity (see Henrard 1970 and Henrard and Roels 1974 for a detailed explanation). Thus, since $\epsilon \ll 1$, we can suppose that both sets of solutions are approximately the same. In other words, using the adiabatic approximation, the new action-angle variables (J_1^*, θ_1^*) are determined up to order ϵ, and this parameter defines the degree of precision of the method.

2.2.1. Solution for the first degree of freedom. Let us recall the subsystem (7). Since $\nu_1 \gg \nu_2$ (and so $\nu_1^* \gg \nu_2^*$), and the indices k, l are bounded (recall that Eq. (2) is a truncated series), we can approximate $k\nu_1^* + l\nu_2^* \approx k\nu_1^*$. Therefore,

$$\begin{aligned} J_1 &\simeq \bar{J}_1^* - \frac{\partial}{\partial\theta_1^*}\left(\sum_{i,j}\sum_{k\neq 0}\frac{\sqrt{-1}A_{i,j,k,l}}{k\nu_1^*}(\bar{J}_1^*)^i (J_2^*)^j E^{\sqrt{-1}(k\bar{\theta}_1^* + l\theta_2^*)}\right) \\ \theta_1 &\simeq \bar{\theta}_1^* + \frac{\partial}{\partial J_1^*}\left(\sum_{i,j}\sum_{k\neq 0}\frac{\sqrt{-1}A_{i,j,k,l}}{k\nu_1^*}(\bar{J}_1^*)^i (J_2^*)^j E^{\sqrt{-1}(k\bar{\theta}_1^* + l\theta_2^*)}\right). \end{aligned} \tag{10}$$

The difference between this expression and (7) is also of the order ϵ. We can easily see that (10) can be rewritten as

$$\begin{aligned} J_1 &\simeq \bar{J}_1^* + \frac{\partial}{\partial\theta_1^*}\hat{B}_1(\bar{J}_1^*, \bar{\theta}_1^*; J_2^*, \theta_2^*) \\ \theta_1 &\simeq \bar{\theta}_1^* - \frac{\partial}{\partial J_1^*}\hat{B}_1(\bar{J}_1^*, \bar{\theta}_1^*; J_2^*, \theta_2^*), \end{aligned} \tag{11}$$

where $\hat{B}_1(\bar{J}_1^*, \bar{\theta}_1^*; J_2^*, \theta_2^*)$ is the generating function with fixed (J_2^*, θ_2^*), corresponding to the single-degree-of-freedom Hamiltonian defined by

$$\begin{aligned} \hat{F}(J_1, \theta_1; J_2, \theta_2) &= \sum_{i,k}\left\{\sum_{j,l}A_{i,j,k,l}(J_2)^j E^{\sqrt{-1}l\theta_2}\right\}(J_1)^i E^{\sqrt{-1}k\theta_1} \\ &= \sum_{i,k}\hat{A}_{i,k}(J_1)^i E^{\sqrt{-1}k\theta_1}, \end{aligned} \tag{12}$$

with (J_2, θ_2) fixed.

In other words, if we consider (J_2, θ_2) as slowly changing external parameters, then the calculation of the action-angle variables $(\bar{J}_1^*, \bar{\theta}_1^*)$ of the reduced Hamiltonian (12), expanded only in the first degree of freedom (i.e., with fixed values of J_2, θ_2), is equivalent up to order ϵ to the determination of (J_1^*, θ_1^*) from the complete Hamiltonian (2).

The action $\bar{J}_1^*$ is an invariant of the "frozen" Hamiltonian (12), but not of the full Hamiltonian (2). Since (J_2, θ_2) vary slowly with time, so does $\bar{J}_1^*$, and according to the adiabatic theory, this variation is such that

$$\frac{d\bar{J}_1^*}{dt} \sim \epsilon^2. \tag{13}$$

Then, for very small values of ϵ this second order variation can be neglected, and the resulting "constant" value of $\bar{J}_1^*$ is called an *adiabatic invariant* of Hamiltonian (2). It is worth noting that these second order corrections to the adiabatic invariant are periodic with the same period of (J_2, θ_2). Thus, they could be eliminated by a suitable averaging of J_1^* over a period of (J_2, θ_2). As we see below, averaging the corrections provides a better approach to the adiabatic invariant than neglecting them.

2.2.2. Solution for the second degree of freedom. We now have expressions for the action-angle variables $J_1^* = J_1^*(J_2^*, \theta_2^*)$ and $\theta_1^* = \theta_1^*(J_2^*, \theta_2^*)$ (determined up to order ϵ) corresponding to the first degree of freedom. Let us pass to the second one. We recall the second half of system (3) as

$$\begin{aligned} J_2 &= J_2^* + \partial B_1/\partial\theta_2^* \\ \theta_2 &= \theta_2^* - \partial B_1/\partial J_2^*. \end{aligned} \tag{14}$$

Introducing the solution of (J_1^*, θ_1^*) into the generating function (4), we have

$$\begin{aligned} B_1' = -\sqrt{-1}\sum_{i,j}\sum_{k,l\neq 0}&\frac{A_{i,j,k,l}}{k\nu_1^* + l\nu_2^*} \\ &\times (J_1^*(J_2^*, \theta_2^*))^i (J_2^*)^j E^{\sqrt{-1}(k\theta_1^*(J_1^*, J_2^*) + l\theta_2^*)}. \end{aligned} \tag{15}$$

We write B_1' instead of B_1 because (once again) there is a difference of order ϵ from the hypothesis of adiabatic approximation.

Explicitly, system (14) can be written as

$$J_2 = J_2^* - \frac{\partial}{\partial \theta_2^*}\left(\sum_{i,j} \sum_{k,l\neq 0} \frac{\sqrt{-1}A_{i,j,k,l}}{k\nu_1^* + l\nu_2^*} \times (J_1^*(J_2^*, \theta_2^*))^i (J_2^*)^j E^{\sqrt{-1}(k\theta_1^*(J_1^*, J_2^*)+l\theta_2^*)} \right)$$
$$\theta_2 = \theta_2^* + \frac{\partial}{\partial J_2^*}\left(\sum_{i,j} \sum_{k,l\neq 0} \frac{\sqrt{-1}A_{i,j,k,l}}{k\nu_1^* + l\nu_2^*} \times (J_1^*(J_2^*, \theta_2^*))^i (J_2^*)^j E^{\sqrt{-1}(k\theta_1^*(J_1^*, J_2^*)+l\theta_2^*)} \right), \tag{16}$$

which corresponds to a one-degree-of-freedom nonautonomous system, since θ_1^* is a linear function of time.

Let us now define the averaging as

$$\langle X \rangle_{\theta_1^*} = \frac{1}{2\pi} \int_0^{2\pi} X \, d\theta_1^* \tag{17}$$

and apply it to both sides of (16). To first order in ϵ, this yields

$$\langle J_2 \rangle_{\theta_1^*} = J_2^* - \frac{\partial}{\partial \theta_2^*}\left(\sum_{i,j} \sum_{l\neq 0} \frac{\sqrt{-1}A_{i,j,0,l}}{l\nu_2^*} \times (J_1^*(J_2^*, \theta_2^*))^i (J_2^*)^j E^{\sqrt{-1}l\theta_2^*} \right)$$
$$\langle \theta_2 \rangle_{\theta_1^*} = \theta_2^* + \frac{\partial}{\partial J_2^*}\left(\sum_{i,j} \sum_{l\neq 0} \frac{\sqrt{-1}A_{i,j,0,l}}{l\nu_2^*} \times (J_1^*(J_2^*, \theta_2^*))^i (J_2^*)^j E^{\sqrt{-1}l\theta_2^*} \right), \tag{18}$$

which corresponds to a one-degree-of-freedom autonomous system.

2.2.3. Reduction to the averaged Hamiltonian. Let us now return to our initial expansion of the Hamiltonian

$$F(J, \theta) = \sum_{i,j,k,l} A_{i,j,k,l} (J_1)^i (J_2)^j E^{\sqrt{-1}(k\theta_1 + l\theta_2)}, \tag{19}$$

and let us introduce the solution to the first degree of freedom $J_1 = J_1(t, J_2, \theta_2), \theta_1 = \theta_1(t, J_2, \theta_2)$. Furthermore, let us average the resulting expression with respect to θ_1 and call this new function $\tilde{F}$. Thus,

$$\tilde{F}(J_2, \theta_2) = \frac{1}{\tau_1^*} \int_0^{\tau_1^*} \sum_{i,j,k,l} A_{i,j,k,l} (J_1)^i (J_2)^j E^{\sqrt{-1}(k\theta_1 + l\theta_2)} \, dt, \tag{20}$$

where $\tau_1^* = 2\pi/\nu_1^*$. Comparing this with system (18), we can see that the action-angle variables (J_2^*, θ_2^*) can be thought of as action-angle variables of the one-degree-of-freedom system defined by the Hamiltonian $\tilde{F}$, if calculated in terms of the *averaged* variables: $\tilde{F}(\langle J_2 \rangle_{\theta_1^*}, \langle \theta_2 \rangle_{\theta_1^*})$.

In other words, we can average the original Hamiltonian (19) over a reference orbit of the first degree of freedom (which is obtained by adiabatic approximation assuming that the second degree is fixed), and then we can use this averaged Hamiltonian to solve the second degree of freedom.

2.3. Extension to Many Degrees of Freedom

The procedure described above does not need to be restricted to two degrees of freedom. Imagine a general case with N degrees of freedom $(J_1, J_2, \ldots, J_N, \theta_1, \theta_2, \ldots, \theta_N)$, such that the unperturbed frequencies ν_i of each angular variable θ_i are finite and large, and satisfy the condition of adiabatic invariance with respect to the previous one. In other words, let us call $\epsilon_{i,j} = \nu_j/\nu_i$ and let us suppose that $\nu_1 \gg \nu_2 \gg \cdots \gg \nu_N$. Once again, the first degree is much faster than the second, the second much faster than the third, an so on. Then, we can repeat the above procedure. First, we solve the Hamiltonian F for (J_1^*, θ_1^*) assuming $(J_2^*, \theta_2^*, \ldots, J_N^*, \theta_N^*)$ fixed (adiabatic approximation). We use this solution to average F over θ_1^* obtaining $\bar{F}$, we solve $\bar{F}$ for (J_2^*, θ_2^*) assuming $(J_3^*, \theta_3^*, \ldots, J_N^*, \theta_N^*)$ fixed, and we use this solution to average $\bar{F}$ over θ_2^* obtaining $\bar{\bar{F}}$, etc.

We can conclude that a general N-degree-of-freedom Hamiltonian system in which the different degrees of freedom are well separated in periods can be approached and solved one degree of freedom at a time. We solve a cascade of single-degree-of-freedom Hamiltonians, each of them averaged over the faster degrees of freedom and with fixed values of the slower degrees of freedom. The consequence of this is twofold. First, as in usual perturbation techniques, the modeling does not need to be done at once over all the dimensions of the problem, with the resulting simplification. Second, for each degree of freedom, the "unperturbed" Hamiltonian used to determine the action-angle variables is much more complete than in the usual perturbation theories. On the other hand, there is a price to be paid: The accuracy of the approximate action-angle variables is directly proportional to ϵ.

3. APPLICATION TO THE TROJAN ASTEROIDS

Let us now apply this method to the case at hand. Although the present work is semianalytical in nature, the procedure we adopted for the evaluation of the proper elements requires an explicit expression for the Hamiltonian (averaged over short-period terms) for a massless body located in tadpole orbits in the vicinity of equilateral Lagrange points. This, in turn, implies finding an expansion of the averaged disturbing function in terms of an appropriate set of variables.

It is worthwhile mentioning that, although significant efforts have been undertaken to find expansions for mean-motion

resonances p/q with $p \neq q$, the same is not true in the case of the Trojans. Practically all the analytical studies of the 1 : 1 resonance use either variational equations or expansions in Cartesian coordinates (x, y, z) centered at the Lagrange points. This occurs because the equilibrium solutions are easier to represent as fixed points in the (x, y, z) space, and also because the disturbing function in Cartesian coordinates is extremely simple and does not have the limitations of the Laplacian-type expansions, which are not convergent in the Trojan case.

Although models based on Cartesian coordinates can yield precise results, they are not suitable for the determination of proper elements. For this purpose, it is better to use an expansion of the disturbing function in terms of orbital elements (or their canonical counterparts). An example of this kind of expansion was recently given by Morais (1999), and it is based on a local expansion around the resonant semimajor axis. Nevertheless, local expansions are not new. Woltjer (1924) devised an *asymmetric* expansion for the Trojans, although it seems that this work has been forgotten for almost 80 years. In the next section we present an alternative expansion which is, in many ways, similar to these.

3.1. The Hamiltonian for the 1 : 1 Resonance

The first step in the expansion of the disturbing function consists in the choice of an adequate set of variables for the nonaveraged system. We adopt the following set

$$\begin{array}{ll} \sigma = \lambda - \lambda_1; & L \\ \varpi; & W = G - L \\ \Omega; & T = H - G \\ \lambda_1; & \Lambda, \end{array} \tag{21}$$

where λ is the mean longitude, ϖ the longitude of perihelion, and Ω the longitude of the ascending node. Elements belonging to the perturber will be designated with a subscript 1. The mean longitude of the planet, λ_1, is a short-period angle, and will therefore be eliminated during the first averaging process. The canonical conjugates W, T are written above in terms of the usual Delaunay variables, and Λ is the conjugate to λ_1.

We believe variables (21) are the best choice for the elaboration of a model of proper elements, mainly because the main frequencies of each angular variable, namely $\nu_\sigma, \nu_\varpi, \nu_\Omega$, are well separated from each other. An example of this property, which is the key piece of this work, is shown in Fig. 1. In this way, it is possible to introduce the adiabatic approach to the problem, defining the parameters $\epsilon_{12} = \nu_\varpi/\nu_\sigma, \epsilon_{23} = \nu_\Omega/\nu_\varpi$, and $\epsilon_{13} = \nu_\Omega/\nu_\sigma$, which are all very small.

Another advantage of variables (21) is due to the fact that, in the planar–circular problem, ϖ and Ω practically do not show periodic variations associated with the libration period of σ. This becomes very important when we perform the canonical transformation to obtain the action-angle variables of the planar–circular problem, as we show below.

In terms of variables (21), the Hamiltonian of the restricted three-body problem, in the extended phase space, can be written as

$$F = -\frac{\mu^2}{2L^2} - n_1 L + n_1 \Lambda - \mu R, \tag{22}$$

where R is the disturbing function, n_1 is the perturber's mean motion, and $\mu = k^2$, this last denoting Gauss's constant.

3.2. Local Variables and Jupp's Transformation

In order to apply the averaging method described in Section 2, we need to have an explicit expression for the Hamiltonian F in terms of nonresonant angular variables. Unfortunately, this is not the case with Eq. (22), because σ is in fact a resonant angle and its unperturbed frequency is close to zero. So, our first step should be to find a canonical transformation from $(L, W, T, \sigma, \varpi, \Omega)$ to new variables $(J, \bar{W}, \bar{T}, \theta, \bar{\varpi}, \bar{\Omega})$ where all the angles are nonresonant.

We begin with the first degree of freedom, associated with the subset (L, σ). First, we split the Hamiltonian function in the form

$$F = F_0(L, W, \sigma) + F_1(L, W, T, \sigma, \varpi, \Omega). \tag{23}$$

Here, F_0 is simply the Hamiltonian of the circular–planar case (for which $T = 0$), and F_1 contains the remaining terms (including the dependence on the perturber's orbital elements, which is implicit). Let us solve this "unperturbed" Hamiltonian F_0 and search for its action-angle variables. Usually this could be done via an averaging process such as Hori's method. But the fact that σ has an unperturbed frequency close to zero makes this impossible, even though F_0 is a single-degree-of-freedom system. Let us recall that classical averaging methods are not valid when a resonant angle exists, and in such cases one usually uses numerical algorithms (e.g., Henrard 1990, Morbidelli and Moons 1993, 1995) to obtain the action-angle variables of F_0. However, this has the drawback of being very CPU-time consuming (especially when this result has to be further introduced into the remaining degrees of freedom at F_1) and does not explicitly yield the proper element associated with this degree of freedom.

Here we choose a different approach which, to our understanding, has several advantages. This approach is based on a canonical transformation originally devised by Jupp (1969, 1970) for the case of the ideal resonance problem. The idea is as follows. Let us think about the libration region of a resonance as a set of invariant curves around a center (i.e., the libration point). If we only concentrate on this region and disregard the structure of the phase space outside the separatrix, we can think of these orbits as (distorted) circulations around a center which is displaced from the origin of the coordinate system. Now, if we find a canonical transformation $(L, \sigma) \to (J, \theta)$ that is simply a translation of the origin to the libration center, we will obtain a new angle θ having a frequency different from zero, and the

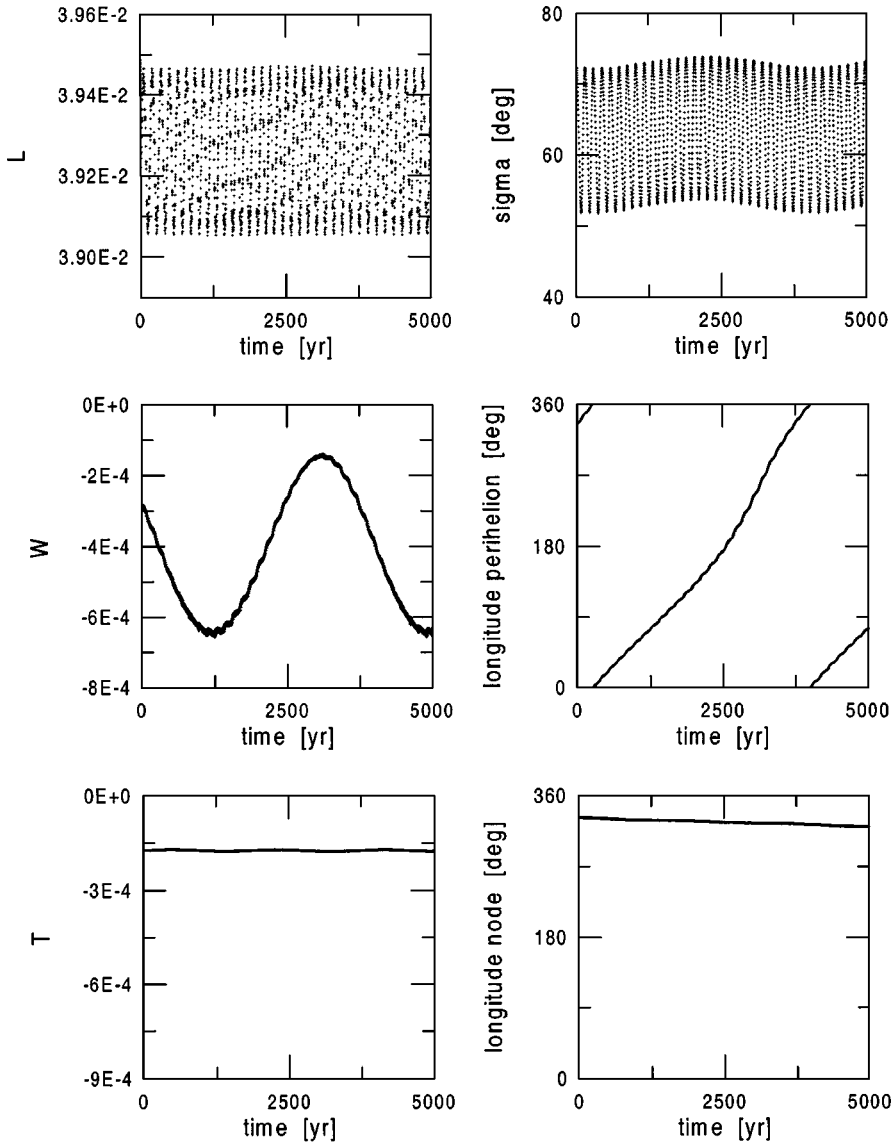

FIG. 1. Numerical simulation of *(659) Nestor* over 5000 years. The different periods of each degree of freedom are noticeable.

integral of J along any orbit will be the action of that trajectory. In other words, we will have an angle σ that librates transformed into another angle θ that circulates. These new variables will have properties of being "nonresonant" (even though they are a simple translation), and we can use an averaging method to determine the action-angle variables.

Although there are many ways of determining (J, θ), possibly the simplest consists of a series of transformations,

$$\begin{aligned}(L, \sigma) &\rightarrow (K, H) = \sqrt{2L}(\cos\sigma, \sin\sigma)\\ (K, H) &\rightarrow (X, Y) = (K - K_c, H - H_c)\\ (X, Y) &= \sqrt{2J}(\cos\theta, \sin\theta) \rightarrow (J, \theta),\end{aligned} \tag{24}$$

where $(K_c, H_c) = \sqrt{2L_c}(\cos\sigma_c, \sin\sigma_c)$ marks the center of libration corresponding to a predetermined value $W = W^0$ given by the initial conditions (remember that W becomes an integral of motion in the F_0 approximation).[2] The values of (L_c, σ_c) are nothing but the equilibrium points of F_0 and can be easily obtained numerically.

For the present work we choose a transformation different from (24) which, although a bit more complicated (because it can no longer be thought of as a simple translation) is still based on the same idea. The change of variables is represented by the relationship

$$\begin{aligned}X &= \Gamma^{-1/2}\left(\hat{K} - \left(K_c^2 - \hat{H}^2\right)^{1/2}\right)\\ Y &= \Gamma^{1/2}\hat{H},\end{aligned} \tag{25}$$

[2] Note that H here is not the classical Delaunay variable.

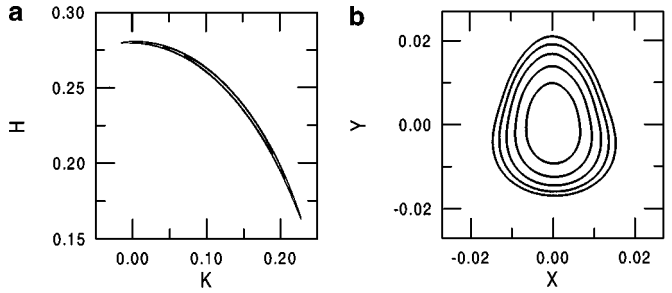

FIG. 2. Transformation to local variables as defined by Eq. (25). (a) Group of five invariant curves of the planar circular problem, corresponding to librations around L_4. (b) Same invariant curves, in terms of the new (X, Y) variables.

where $(\hat{K}, \hat{H}) = \sqrt{2L}(\cos(\sigma - \sigma_c), \sin(\sigma - \sigma_c))$ and $\Gamma = \Gamma(K_c)$ is a scaling factor which modifies the shape of the trajectories. This transformation is canonical and is valid as long as $|\sigma_{\max} - \sigma_c| < \pi/2$ (with both $\sigma_{\max}$ and σ_c defined between $\pm\pi$). It is worth noting that all the known real Trojans fulfill this condition. An example of the relation between these two sets of variables is given in Fig. 2. On the left plot we show a number of invariant curves (obtained numerically) as they appear in regular resonant variables (K, H). On the right plot, we have the same orbits, but this time they are shown after the transformation to (X, Y). Since the transformation is an explicit function of the center of libration, we call them *local variables*.

By means of this very simple and purely geometrical "banana-to-pear" transformation, we are able to bypass the difficulties generated by the libration of σ, and define variables suitable for the application of a classical averaging method. Equation (25) involves only the first degree of freedom, and in order to extend and complete the canonical transformation to the other degrees of freedom, we make use of the corrections introduced by Henrard (1990). Thus, our new set of variables $(J, \bar{W}, \bar{T}, \theta, \bar{\varpi}, \bar{\Omega})$ is such that

$$\begin{aligned} L &= L(J, \bar{W}, \bar{T}, \theta) \\ \sigma &= \sigma(J, \bar{W}, \bar{T}, \theta) \\ W &= \bar{W} \\ \varpi &= \bar{\varpi} + \rho_1(J, \bar{W}, \bar{T}, \theta) \\ T &= \bar{T} \\ \Omega &= \bar{\Omega} + \rho_2(J, \bar{W}, \bar{T}, \theta), \end{aligned} \tag{26}$$

where functions ρ_1 and ρ_2 are given by

$$\begin{aligned} \rho_1 &= \int_0^\theta \left(\frac{\partial\sigma}{\partial W}\frac{\partial L}{\partial\theta} - \frac{\partial\sigma}{\partial\theta}\frac{\partial L}{\partial W} \right) d\theta \\ \rho_2 &= \int_0^\theta \left(\frac{\partial\sigma}{\partial T}\frac{\partial L}{\partial\theta} - \frac{\partial\sigma}{\partial\theta}\frac{\partial L}{\partial T} \right) d\theta. \end{aligned} \tag{27}$$

As we have mentioned, one important consequence of our choice of angular variables (Eq. 21) is that ρ_1 and ρ_2 are practically zero. This is because the frequency of σ does not have any significant contribution to the power spectra of ϖ and Ω. Thus, we can consider the equalities $\varpi = \bar{\varpi}$ and $\Omega = \bar{\Omega}$ without introducing any important error in the transformation. Nevertheless, in order to guarantee the internal consistency of the transformation, we will maintain the canonical corrections ρ_1 and ρ_2 in our calculations. In order to simplify the notation, we use the set (W, T, ϖ, Ω) instead of $(\bar{W}, T, \bar{\varpi}, \bar{\Omega})$.

Now, using transformation (26), it is possible to write (23) in the form

$$F = F_0(J, W, \theta) + F_1(J, W, T, \theta, \varpi, \Omega). \tag{28}$$

It is worth recalling that the set $(J, W, T, \theta, \varpi, \Omega)$ is canonical by construction, and that θ is a circulating angle with frequency $\nu_\theta = \nu_\sigma$.

3.3. The Asymmetric Expansion of the Hamiltonian

Having specified a complete set of canonical variables $(J, W, T, \theta, \varpi, \Omega)$ suitable for the averaging process, the next step is the explicit construction of the Hamiltonian of the system (28). For this purpose we will adopt the approximation given by the so-called asymmetric expansion of the disturbing function. This kind of seminumeric expansion is local in nature. It was first developed by Ferraz-Mello and Sato (1989) for planar mean motion resonances of the type $(p + q)/p$, and it has shown a remarkable efficiency in numerous studies of the dynamics of main belt asteroids. A version of this expansion for the spatial resonant case was developed by Roig *et al.* (1998), and in this section we follow the main outlines of that work. However, it should be mentioned that the method of obtaining the asymmetric expansion in the Trojan case is somewhat different from the one used in previous resonant cases. We give here a brief summary of the corresponding calculations.

Recalling Eq. (22), we begin by writing

$$R = \frac{m_1}{a_1}(f + f'), \tag{29}$$

where f is the direct part of the disturbing function, and f' is the indirect contribution. Here m_1 is the mass of the perturbing planet, and a_1 is its semimajor axis. Other orbital elements introduced throughout this section are: eccentricity (e), inclination with respect to the invariable plane (I), true anomaly (v), eccentric anomaly (u), and mean anomaly (M). As before, the orbital elements of the perturbing planet (in this case Jupiter) are denoted with a subscript 1. Explicitly, we have

$$\begin{aligned} f &= b^{-1/2} \\ f' &= -\left(\frac{a_1}{r_1}\right)^2 \left(\frac{r}{a_1}\right) \cos\Phi \end{aligned} \tag{30}$$

with

$$b = \left(\frac{r}{a_1}\right)^2 + \left(\frac{r_1}{a_1}\right)^2 - 2\left(\frac{r_1}{a_1}\right)\left(\frac{r}{a_1}\right)\cos\Phi, \qquad (31)$$

where r denotes the modulus of the instantaneous position vector, and Φ is the angle between r and r_1. Since we are considering the spatial case, $\cos\Phi$ can be written as the sum of six periodic terms,

$$\cos\Phi = \sum_{i=0}^{5} \alpha_i \cos\Phi_i, \qquad (32)$$

where the coefficients α_i are functions of the sine of half the inclinations (i.e., $\eta = \sin I/2$),

$$\begin{aligned}
\alpha_0 &= 1 - \eta^2 - \eta_1^2 + \eta^2\eta_1^2 \\
\alpha_1 &= \left(1 - \eta_1^2\right)\eta^2 \\
\alpha_2 &= 2\eta\eta_1(1-\eta^2)^{1/2}\left(1-\eta_1^2\right)^{1/2} \\
\alpha_3 &= -\alpha_2 \\
\alpha_4 &= (1-\eta^2)\eta_1^2 \\
\alpha_5 &= \eta^2\eta_1^2,
\end{aligned} \qquad (33)$$

and the arguments are

$$\begin{aligned}
\Phi_0 &= v - v_1 + \varpi - \varpi_1 \\
\Phi_1 &= v + v_1 + \varpi + \varpi_1 - 2\Omega \\
\Phi_2 &= v - v_1 + \varpi - \varpi_1 - \Omega + \Omega_1 \\
\Phi_3 &= v + v_1 + \varpi + \varpi_1 - \Omega - \Omega_1 \\
\Phi_4 &= v + v_1 + \varpi + \varpi_1 - 2\Omega_1 \\
\Phi_5 &= v - v_1 + \varpi - \varpi_1 - 2\Omega + 2\Omega_1.
\end{aligned} \qquad (34)$$

3.3.1. Expansion in terms of the planet's elements. We begin our expansion with a Taylor series of (29) with respect to e_1 and η_1 (centered at $e_1 = \eta_1 = 0$) up to the third order in e_1 and second order in η_1. Let us recall that, in the case of Jupiter, $e_1 \approx 0.05$ and $\eta_1 \approx 0.005$. The extension to the third order in eccentricity proved to be necessary for the bodies with an extremely long period of oscillation of the longitude of node, such as (*617*) *Patroclus*. The procedure closely follows the calculations performed by Roig *et al*. (1998), although there are significant differences due to the fact that in our case $\eta \neq 0$. We can write our disturbing function in the form

$$R = \frac{m_1}{a_1}\sum_{i=0}^{3}\sum_{j=0}^{2} R_{i,j}(e_1)^i(\eta_1)^j, \qquad (35)$$

where $R_{i,j} = f_{i,j} + f'_{i,j}$, and

$$f_{i,j} = \left.\frac{\partial^{i+j} f}{\partial e_1^i \partial \eta_1^j}\right|_{e_1=\eta_1=0;\eta\neq 0}; \quad f'_{i,j} = \left.\frac{\partial^{i+j} f'}{\partial e_1^i \partial \eta_1^j}\right|_{e_1=\eta_1=0;\eta\neq 0}. \qquad (36)$$

The dependence of the disturbing function on η_1 appears directly through $\cos\Phi$. However, the dependence on e_1 appears through r_1 and v_1. Then, in order to calculate the derivatives, we use the second order expansions in mean anomaly:

$$\begin{aligned}
r_1 &= a_1\left[1 - e_1\cos M_1 + \frac{1}{2}e_1^2(1-\cos 2M_1) + \cdots\right] \\
v_1 &= M_1 + 2e_1\sin M_1 + \frac{5}{4}e_1^2\sin 2M_1 + \cdots
\end{aligned} \qquad (37)$$

After a lot of cumbersome algebra, including writing the dependence on the angular variables ϖ_1 and Ω_1 explicitly, the resulting expression, written in complex form, is given by

$$R = \frac{m_1}{a_1}\sum_{i,j}\sum_{r=-3}^{3}\sum_{s=-2}^{2} R_{i,j,r,s}(e_1)^i(\eta_1)^j E^{\sqrt{-1}(r\varpi_1 + s\Omega_1)}, \qquad (38)$$

where the new complex coefficients $R_{i,j,r,s}$ are functions of M_1 (i.e., of λ_1) and of all the orbital elements of the massless body.

3.3.2. Expansion in terms of the asteroid's elements. Let us now see the expansion of $R_{i,j,r,s}$ in terms of the orbital variables of the massless body. We introduce the following transformations from true to eccentric anomaly:

$$\begin{aligned}
\Psi_1 &= \frac{r}{a_1}\cos v = \frac{a}{a_1}(\cos u - e) \\
\Psi_2 &= \frac{r}{a_1}\sin v = \frac{a}{a_1}(1-e^2)^{1/2}\sin u.
\end{aligned} \qquad (39)$$

Then, the position of the massless particle can be expressed in terms of these quantities as

$$\begin{aligned}
\left(\frac{r}{a_1}\right)^2 &= \Psi_1^2 + \Psi_2^2 \\
\frac{r}{a_1}E^{\pm\sqrt{-1}v} &= \Psi_1 \pm \sqrt{-1}\Psi_2,
\end{aligned} \qquad (40)$$

and this allows us to write the coefficients as $R_{i,j,r,s} = R_{i,j,r,s}(\Psi_1, \Psi_2, \eta, \sigma, \varpi, \Omega, \lambda_1)$. Now, according to the usual asymmetric expansion of the disturbing function, we should proceed with a Taylor series in (a, e, η), which could be obtained explicitly and by using the above relations (see Roig *et al*. 1998 for details). However, we found it more convenient to work directly with an expansion in canonical variables (i.e., momenta) than with orbital elements. Although the algebra becomes more complicated, this will lead to a great simplification in the subsequent analysis of our results.

In order to obtain the derivatives directly in the canonical momenta (J, W, T), we use the chain rule and define

$$R_{i,j,k,l,m,r,s} = \frac{\partial^{k+l+m} R_{i,j,r,s}}{\partial (J^{1/2})^k \partial W^l \partial T^m}. \quad (41)$$

It is worth noting that these derivatives are not evaluated at the origin. In particular, the derivatives with respect to J are evaluated at the condition $J = 0$, which, in fact, corresponds to the libration point (K_c, H_c) used in the transformation (25). Moreover, the derivatives with respect to (W, T) are evaluated at predetermined values (W_0, T_0) different from zero. This is mandatory because the structure of the phase space of the Trojan problem could not be well reproduced with a low order Taylor series centered at the origin of eccentricities and inclinations. The main cause of this is the proximity of the libration points to the collision curve of the planar problem ($T = 0$). The collision curve (i.e., the set of points in the phase space where a collision between the asteroid and the perturbing planet can happen) constitutes an intrinsic singularity of any expansion of the disturbing function (in powers of T) around $T = 0$. Then, the use of such an expansion in the case of the $1/1$ resonance makes the equilibrium points lie very close to an essential singularity of the disturbing function. As a consequence, the structure of the phase space represented by an expansion around $W_0 = T_0 = 0$ could be very different from that of the real system, especially taking into account that real Jupiter Trojans have moderate to large eccentricities and inclinations.

In this way, we write the expansion of the disturbing function as

$$R = \sum_{i,j} \sum_{r,s} \sum_{k,l,m=0}^{3} \sum_{n,p,q=-3}^{3} R_{i,j,k,l,m,n,p,q,r,s}(W_0, T_0) \times J^{k/2} W^l T^m (e_1)^i (\eta_1)^j E^{\sqrt{-1}(n\theta + p\varpi + q\Omega + r\varpi_1 + s\Omega_1)}, \quad (42)$$

where the complex coefficients $R_{i,j,k,l,m,n,p,q,r,s}$ also depend on λ_1. In (42), the dependence on angle θ appears explicitly because we make the expansion around $J = 0$. However, the dependence on the other two angles, ϖ and Ω, is obtained through a numerical Fourier analysis, such that

$$R_{i,j,k,l,m,n,p,q,r,s} = \frac{1}{4\pi^2} \int_0^{2\pi} \int_0^{2\pi} R_{i,j,k,l,m,n,r,s}(W_0, T_0, \varpi, \Omega) \times E^{-\sqrt{-1}(p\varpi + q\Omega)} \, d\varpi \, d\Omega. \quad (43)$$

Now, after a suitable averaging over the mean longitude of the perturber, the expansion of the averaged disturbing function $\langle R \rangle$ reads

$$\langle R \rangle = \sum_{i,j} \sum_{r,s} \sum_{k,l,m} \sum_{n,p,q} \tilde{R}_{i,j,k,l,m,n,p,q,r,s} \; J^{k/2} W^l T^m (e_1)^i (\eta_1)^j \times E^{\sqrt{-1}(n\theta + p\varpi + q\Omega + r\varpi_1 + s\Omega_1)}, \quad (44)$$

where

$$\tilde{R}_{i,j,k,l,m,n,p,q,r,s} = \frac{1}{2\pi} \int_0^{2\pi} R_{i,j,k,l,m,n,p,q,r,s} \, d\lambda_1. \quad (45)$$

As a final step, we extend the expansion to include the two-body contribution. In order to do this, we just need to expand the first two sums of Eq. (22), which is a trivial calculation (the third term, $n_1\Lambda$, is a mere constant since $\langle R \rangle$ does not depend on λ_1). In this way, we can finally write the complete expansion of the averaged Hamiltonian for the 1 : 1 resonance as

$$\langle F \rangle = \sum_{i,j,k,l,m} \sum_{n,p,q,r,s} F_{i,j,k,l,m,n,p,q,r,s} \; J^{k/2} W^l T^m (e_1)^i (\eta_1)^j \times E^{\sqrt{-1}(n\theta + p\varpi + q\Omega + r\varpi_1 + s\Omega_1)}, \quad (46)$$

where coefficients $F_{i,j,k,l,m,n,p,q,r,s}$ are constant with respect to all the variables (in the following, we avoid the use of $\langle \; \rangle$ to simplify notation). Needless to say, this expansion is extremely long and cumbersome to calculate, even though formally it is very elegant. Since the degrees of freedom of our particular system are well separated in period, we only need to work with one degree of freedom at a time, as we will see as follows. Then, the whole expansion (46) can be divided into several parts, and in fact, we never need to determine all its coefficients explicitly at once. But the "philosophy" underneath this expansion will be maintained and used throughout this work.

4. THE HIERARCHICAL AVERAGING OF THE HAMILTONIAN

If we consider the case of the restricted three-body problem, that is, assuming Jupiter in a fixed elliptic orbit, then Eq. (46) provides an explicit expression $F(J, W, T, \theta, \varpi, \Omega; e_1, \eta_1, \varpi_1, \Omega_1)$ for the Hamiltonian (the variables of the perturber appear here as external fixed parameters, but we are going to maintain them explicitly). As we mentioned in Section 3.1, the three degrees of freedom in the Trojan case are well separated in frequency. Then, we can introduce the small parameters $\epsilon_{12} = \nu_\varpi/\nu_\theta$, $\epsilon_{23} = \nu_\Omega/\nu_\varpi$ and $\epsilon_{13} = \nu_\Omega/\nu_\theta$, and we can proceed as in Section 2 by treating each degree of freedom separately.

4.1. The Motion of the Trojans on Short Timescales

We begin by fixing values of (W, T, ϖ, Ω) and considering only the behavior of (J, θ). Since the period of ϖ is about 3500 yr, the results presented here are valid only for timescales much smaller than this value. Typical values of the libration period of σ are about 150 yr; thus, we can guarantee that the results will be quantitatively accurate for several complete orbits around the Lagrange point.

Following the calculations of Section 3.3, we perform an asymmetric expansion only in (J, θ). Then, the Hamiltonian

takes the form

$$F = \sum_{i,k} A_{i,k}\ J^{i/2} E^{\sqrt{-1}k\theta}$$
$$= \sum_{i} A_{i,0}\ J^{i/2} + \sum_{i} \sum_{k\neq 0} A_{i,k}\ J^{i/2} E^{\sqrt{-1}k\theta}, \qquad (47)$$

where $A_{i,k} = A_{i,k}(W, T, \varpi, \Omega; e_1, \eta_1, \varpi_1, \Omega_1)$ are constant coefficients. This is an explicit one-degree-of-freedom system in which the angle θ is not resonant. Its solution as a function of time can be found by some numerical or analytical perturbation method. We choose the classical Hori's averaging, where the role of the small parameter is played by the quantity $\varepsilon = |A_{1,1}|/|A_{1,0}|$. Notice that this parameter is not directly related to any of the usual quantities, such as the mass of the perturbing body or the eccentricity or inclination of the planet, but is mainly a weak function of the amplitude of the libration. This is because the first sum in Eq. (47) represents the librational motion around the Lagrange point, and thus it depends on the mass and the elements of the perturbing body. In other words, the "integrable" part of Hamiltonian (47) depends itself on μ, e_1, and η_1. The second term, i.e., the "perturbation," only modifies the shape of the invariant curves in accordance with the true librational orbits.

The averaging of Hamiltonian (47) could be performed up to first or second order in ε, depending on the magnitude of this quantity. In the case at hand, typical values of ε are of the order of 10^{-3}–10^{-2}, and we have carried out the average up to the second order. This procedure yields new action-angle variables (J^*, θ^*) such that θ^* is an angle with constant frequency. Nevertheless, let us recall that these new variables will be functions not only of the initial conditions (J^0, θ^0), but also of the remaining degrees of freedom, i.e.,

$$J^* = J^*(J^0, \theta^0, W, T, \varpi, \Omega; e_1, \eta_1, \varpi_1, \Omega_1)$$
$$\theta^* = \theta^*(J^0, \theta^0, W, T, \varpi, \Omega; e_1, \eta_1, \varpi_1, \Omega_1). \qquad (48)$$

Were it not for this dependence, J^* would be the first proper element of the problem. As we already explained (see Section 2.2.1), the dependence on the other degrees of freedom introduces a periodic correction to J^* (of second order in ϵ_{12}, at least) which we will try to eliminate later by further averaging. The inverse transformation

$$J = J(J^*, \theta^*(t), W, T, \varpi, \Omega; e_1, \eta_1, \varpi_1, \Omega_1)$$
$$\theta = \theta(J^*, \theta^*(t), W, T, \varpi, \Omega; e_1, \eta_1, \varpi_1, \Omega_1) \qquad (49)$$

will give us the evolution of the orbit as a function of time. Finally, inverting the transformation equations (25), we can get (L, σ) also as a function of time.

An example of this can be seen in Fig. 3a. The closed periodic curve plotted with thick lines is the solution for one period of

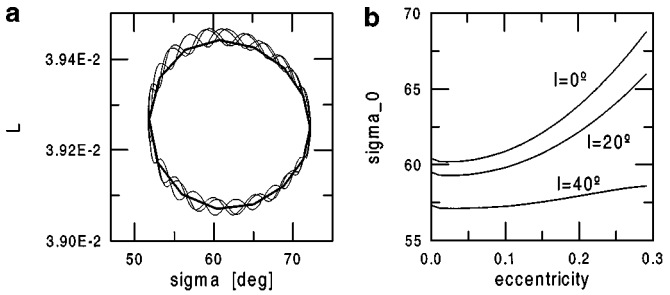

FIG. 3. (a) Numerical simulation of *(659) Nestor* over 500 years (dots) versus model (thick curve). (b) Variation of the libration center for zero-amplitude solutions as a function of the eccentricity and inclination. *Nestor* is located at $e \simeq 0.13$ and $I \simeq 5^\circ$.

libration, obtained from (49) in the case of (*659*) *Nestor*. The dots surrounding this curve are the result of a numerical integration of that asteroid over 500 yr in the framework of the spatial–elliptic restricted three-body problem, using the well known RA15 integrator (Everhart 1985). The "loops" observed on both sides of the thick curve are short period variations associated with Jupiter's orbital motion. An interesting feature that can also be appreciated in Fig. 3 is that the "geometrical" center of the librational trajectory occurs at a value of $\sigma_0 \simeq 62^\circ$, that is displaced with respect to the L_4 fixed point. This is in part due to the finite amplitude of libration, but it is also related to the nonzero values of the eccentricities and inclinations (see Namouni and Murray 2000 for a detailed study). Using our Hamiltonian (47), we can reproduce this behavior directly by searching for the fixed points in the (L, σ) space for different values of e and I (or equivalently, of W and T). The result is shown in Fig. 3b. We can see that the value of σ_0 increases with increasing eccentricity, but on the other hand, it is smaller at larger values of the inclination. It is worth noting that the curves in Fig. 3b were calculated for zero-amplitude orbits, and they should slightly shift upwards when solutions with nonzero amplitude are considered. As an example, (*659*) *Nestor* has $D \simeq 10^\circ$, $e \simeq 0.13$, and $I \simeq 5^\circ$, which implies $\sigma_0 \simeq 62^\circ$.

We wish to stress the fact that our approach has some advantages with respect to the usual perturbative methods applied to resonant systems. First, with these latter methods, the intermediate Hori's kernel is the restricted circular–planar problem or, eventually, its approximation by an Andoyer Hamiltonian (Ferraz-Mello, in preparation). On the other hand, the kernel of our method is somewhat more complete, because it already contains information about the adopted eccentricity of the perturber and the inclinations. Moreover, as we see below, it also contains information about the direct perturbation of nonresonant planets.

The consequence of using a more complete kernel is shown in Fig. 4. The thin curve represents the temporal variation of σ for (*659*) *Nestor*, obtained from a numerical integration of the restricted planar elliptic problem, using RA15. The thin horizontal line is the libration center σ_c, as determined from the circular–planar problem. The bold curve is the value of the

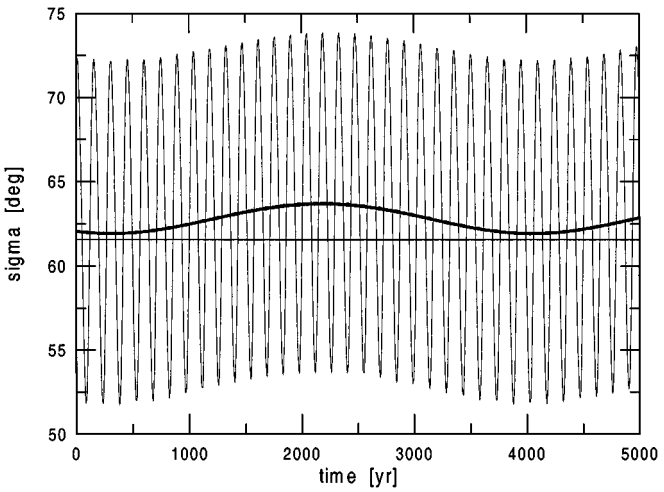

FIG. 4. Numerical simulation of σ for (*659*) *Nestor* (thin curve). The horizontal line corresponds to the equilibrium value σ_c as determined by the planar–circular problem. The thick curve is $\sigma_0(W, T, \varpi, \Omega)$, as determined from our model.

libration center σ_0 as obtained from our method, which is not a constant. Indeed, it has a variation associated with the motion of (W, ϖ) forced by the eccentricity of Jupiter. It is clear that the mean value of σ_0 provides a better approximation to the time average of σ than the value of σ_c, which strongly depends on the adopted value for W.

A second advantage of our method is related to Jupp's transformation. In classical approaches, the action-angle variables of the kernel are calculated, and the libration "banana" is transformed into a circle. Consequently, the information about the phase of the resonant angle is lost, and it becomes very difficult to relate the radius of the circle with the amplitude of libration. On the other hand, in the transformation $(L, \sigma) \to (J, \theta)$ we keep the information about the phase, since the maximum and minimum values of σ are directly related to the conditions $\theta = \pm\pi/2$.

On the other hand, we have to note that our method has a limitation which is common to all the perturbative methods based on Lie series in the small parameter. Due to the local character of Jupp's transformation, we would expect some significant loss of accuracy for those orbits very close to the separatrix of motion. Fortunately, all real Trojans lie far away from the separatrix, and we verify below that, for these objects, our second order average over the first degree of freedom is more than adequate.

Another limitation of our method involves the orbits with a rather high inclination but an extremely small amplitude of libration. Since our transformation to local variables is based on the equilibrium points of the planar Hamiltonian, it happens that the "local" center does not coincide with the "true" center of libration for highly inclined orbits (recall Fig. 3b). Then we could expect the occurrence of a vicious case when the difference between the local and true centers is larger than the actual amplitude of libration of the trajectory. In this case, the libration is only transformed into "another" libration, becoming intractable by our method. Fortunately (once again), no real Trojan falls in this category.

4.2. The Motion of the Trojans on Long Timescales

Let us now solve the two remaining degrees of freedom. Proceeding as in Section 2.2.2, we introduce the solution (49) into the complete Hamiltonian and average (up to the second order) over a period of θ^* (recall Eq. 20). Let us call this new Hamiltonian $\bar{F}$. Again, by means of an asymmetric expansion as described in Section 3.3, we expand $\bar{F}$ only in (W, T, ϖ, Ω), getting

$$\bar{F} = \sum_{i,j,k,l} A_{i,j,k,l} W^i T^j E^{\sqrt{-1}(k\varpi + l\Omega)}, \tag{50}$$

where $A_{i,j,k,l} = A_{i,j,k,l}(e_1, \eta_1, \varpi_1, \Omega_1)$ are constant coefficients. It is worth noting that each of these coefficients has already embedded the averaging over the libration period τ^*_θ. Hamiltonian (50) corresponds to a two-degrees-of-freedom system.

At this point, we can proceed in two ways: Either we take advantage of the hierarchical separation and work with each canonical pair, (W, ϖ) and (T, Ω), separately; or we work with both degrees of freedom simultaneously. Which approach we choose depends on what aspect of the dynamics we are currently interested in. In the following, we show examples of both approaches.

4.2.1. Adiabatic approach. Let's start with the hierarchical averaging. First, we write Hamiltonian (50) in the form

$$\bar{F} = \sum_{i,k} \hat{A}_{i,k} W^i E^{\sqrt{-1}(k\varpi)}, \tag{51}$$

where $\hat{A}_{i,k} = \sum_{j,l} A_{i,j,k,l} T^j E^{\sqrt{-1}(l\Omega)}$. Since the period of Ω is much longer than that of the longitude of the perihelion (i.e., $\epsilon_{23} = \nu_\Omega/\nu_\varpi \ll 1$), we suppose the pair (T, Ω) to be fixed and treat $\bar{F}$ as a one-degree-of-freedom system, with external slow-varying parameters. Proceeding in the same way as in Section 4.1, the terms that do not depend on the angles are grouped in the "unperturbed" part, and the remaining ones are left to the "perturbation." That is,

$$\bar{F} = \sum_i \hat{A}_{i,0} W^i + \sum_i \sum_{k\neq 0} \hat{A}_{i,k} W^i E^{\sqrt{-1}(k\varpi)}, \tag{52}$$

where, again, the small parameter of the perturbation can be identified with $\varepsilon = |\hat{A}_{1,1}|/|\hat{A}_{1,0}|$. In this case, we apply a first order Hori's averaging, and solve this system to obtain

$$\begin{aligned} W^* &= W^*(W^0, \varpi^0, T, \Omega; e_1, \eta_1, \varpi_1, \Omega_1) \\ \varpi^* &= \varpi^*(W^0, \varpi^0, T, \Omega; e_1, \eta_1, \varpi_1, \Omega_1) \end{aligned} \tag{53}$$

as the new action-angle variables. The inverse transformation yields the evolution of the pair (W, ϖ) valid for timescales a

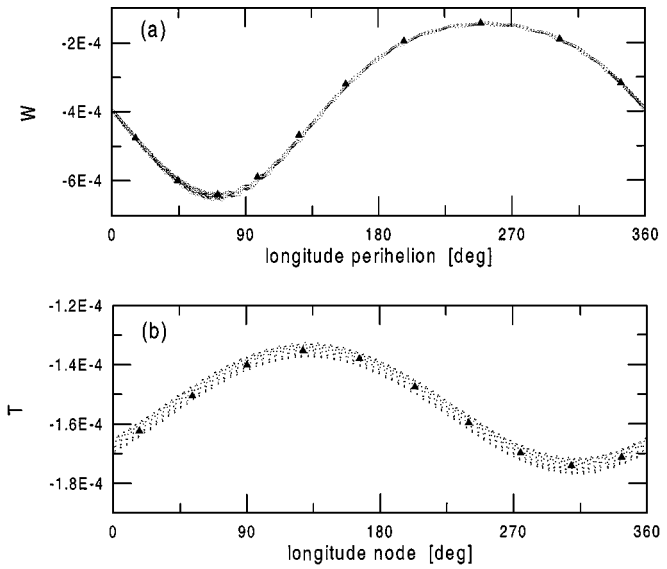

FIG. 5. Long-term evolution of *(659) Nestor.* Dots correspond to numerical simulations of the exact equations of motion over 5,000 yr (a) and 500,000 yr (b) Large symbols correspond to the results obtained with Hamiltonians $\bar{F}$ (top) and $\bar{\bar{F}}$ (bottom).

fraction of the period of Ω. An example is presented in Fig. 5a, which shows the variation of the momentum W as a function of the longitude of perihelion for (*659*) *Nestor*. Small dots indicate the results of a numerical simulation for 5000 yr using RA15. Large symbols correspond to the solution obtained from (53).

The solution for the pair (T, Ω) follows the same procedure. Introducing the inverse of (53) into $\bar{F}$ and averaging up to the first order over a period of ϖ^*, we arrive at a new Hamiltonian $\bar{\bar{F}}(T, \Omega; e_1, \eta_1, \varpi_1, \Omega_1)$. Again, it is separated by grouping terms depending on the angles in the "perturbation." Applying a first order Hori's averaging, we can determine the evolution of the longitude of node and its conjugate momentum T. Figure 5b shows a comparison of this result (large symbols) with a numerical simulation over 500,000 yr (small dots). Figure 5 allows us to conclude that in both cases the agreement between the model and the numerical data is very good.

4.2.2. Simultaneous solution. As mentioned above, Hamiltonian (50) can also be solved by using a first order Hori's averaging over both degrees of freedom simultaneously. Once again, the Hamiltonian is divided so that all the terms depending on the angles (ϖ, Ω) are grouped in the "perturbation." Then, we find a suitable Lie-type generating function B of the canonical transformation $(W, T, \varpi, \Omega) \rightarrow (W^*, T^*, \varpi^*, \Omega^*)$ such that the transformed Hamiltonian $\bar{F}^*$ is a function only of the new momenta: $\bar{F}^*(W^*, T^*)$. The new variables $(W^*, T^*, \varpi^*, \Omega^*)$ will depend solely on the initial conditions and on the orbital elements of the perturber. Inverting them, we obtain (W, T, ϖ, Ω) as functions of time.

In order to test the reliability of this solution we perform the following check. We start by considering a Hamiltonian similar to that of Eq. (50), but instead of performing a second order average over the libration period of σ, we consider only the solutions of zero-amplitude libration. We chose zero-amplitude solutions because we are comparing a single function with a whole population of real bodies, each with different amplitudes of libration.[3] In other words, we evaluate the coefficients $A_{i,j,k,l}$ at fixed values (L_0, σ_0) corresponding to the center of libration. Following Eq. (5), the frequency of ϖ^* is then given by

$$\nu^*_\varpi = \frac{2\pi}{P^*_\varpi} = \frac{\partial \bar{F}^*}{\partial W^*} = \sum_j \left\{ \sum_i i\, A_{i,j,0,0} (W^*)^{(i-1)} \right\} (T^*)^j . \tag{54}$$

Since the coefficient $A_{1,1,0,0}$ dominates by about two orders of magnitude over the remaining $A_{i,1,0,0}$, $i > 1$, then P^*_ϖ will be practically uncoupled with W^* (numerical results by Schubart and Bien 1987 have already shown this behavior)[4]. Then we can evaluate W^* in the above equation at the mean value of the Trojan swarm. Finally, we use the relations (21) to convert T^* to proper inclination I^*, and we can plot $P^*_\varpi(I^*)$. This is shown in Fig. 6a as the thick curve. In Fig. 6, we also show the values of P^*_ϖ I^* obtained from our semianalytical model (small crosses) for 514 known Trojans. We clearly see a marked correlation, especially for higher values of I^* (see Schubart and Bien 1987 for more details). Considering that (54) has been obtained for zero-amplitude orbits, the agreement is very good.

In Fig. 6b we show the same curve $P^*_\varpi(I^*)$, but now the small crosses correspond to the numerical values of $P^*_\varpi \equiv 2\pi/g$ vs I^* as obtained by Milani (1993) for 174 real Trojans (his Table 2). Again, we see the same correlation as before, with the analytic curve overshooting the numerical data, especially at low inclinations. In fact, the overshooting observed in Fig. 6a is likely due to the choice of zero-amplitude solutions, rather than to errors in our proper elements.

We can also use both figures to compare our proper elements with those determined by Milani (1993). For small-to-moderate values of I^* there is practically no observed difference between them (both in the dispersion of the correlation and in the numerical values). For large inclinations, however, it is interesting to note that our model seems to underestimate the value of P^*_ϖ. The difference seems to be directly proportional to the inclination, and could be related to (i) limitations of our model, and/or (ii) long period effects not accounted for in Milani's (1993) simulation (which only spanned 10^6 yr).[5]

[3] Averaged solutions do not lead to a unique result, since they depend on the initial amplitudes of libration.

[4] Note that $A_{1,1,0,0}$ is always larger than the remaining coefficients, but it does not dominate over $A_{1,j,0,0}$, $j > 1$. This translates into a nonlinear dependence of ν^*_ϖ on T^*.

[5] We know that some Trojan asteroids (already detected by Milani 1993) have periods of Ω larger than one million years, and a precise determination of the proper inclinations by means of a numerical Fourier transform needs integrations spanning several periods of Ω.

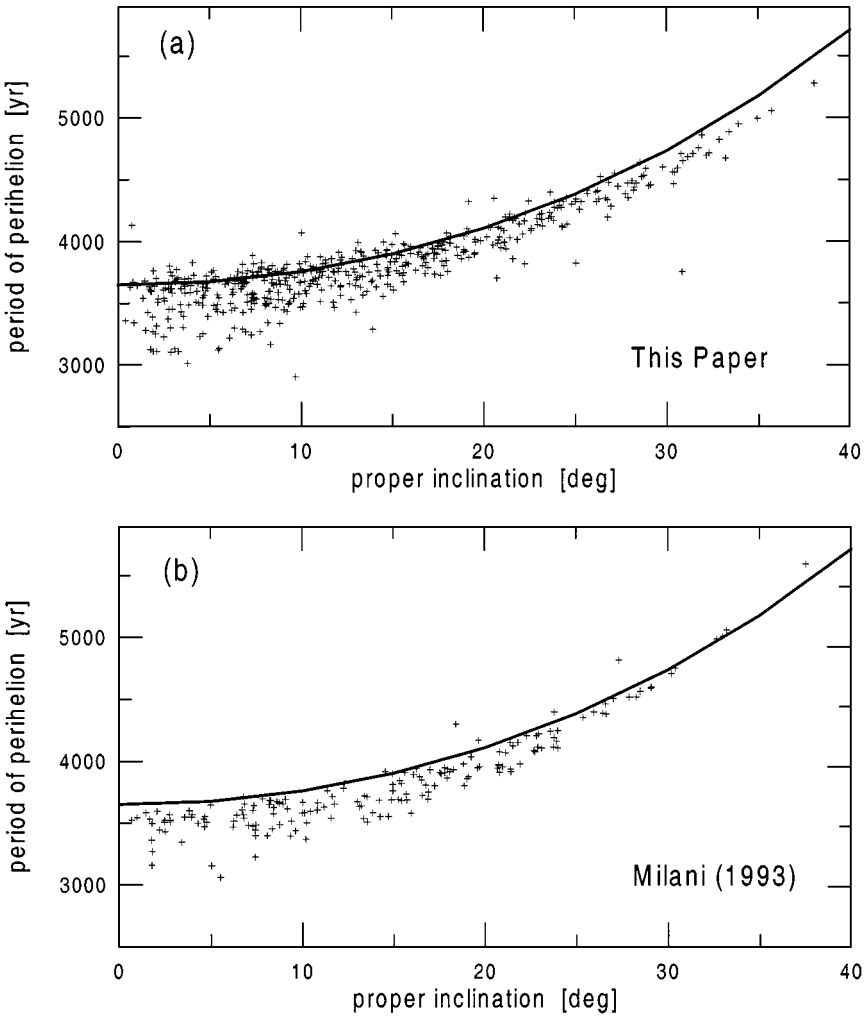

FIG. 6. Period of oscillation of the proper longitude of perihelion as a function of the proper inclination. Crosses are real Trojans; thick lines correspond to our model for zero-amplitude of libration.

4.2.3. Dealing with paradoxal librations of (W, ϖ). For several Trojans, the motion of the longitude of perihelion shows a behavior known as *paradoxal libration*. Earlier theories on the motion of the Trojans (Bien and Schubart 1983; see also Érdi 1988) approximated the evolution of e, ϖ by relations of the type

$$\begin{aligned} k &\equiv e\cos\varpi = A + B\cos gt \\ h &\equiv e\sin\varpi = C + D\sin gt. \end{aligned} \tag{55}$$

The trajectories in the (k, h) plane are ellipses with their center shifted from the origin according to the values of A and C. This displacement is usually known as *forced eccentricity*. A paradoxal libration happens whenever $|A| > |B|$ and/or $|C| > |D|$. In this case, the angle ϖ does not take all the possible values between 0 and 2π, but seems to librate between a maximum and a minimum. Since this libration is not associated with any structure of separatrix, it is called paradoxal.

The possible occurrence of paradoxal librations of ϖ introduces an additional difficulty in the solution of Hamiltonian (50). In these cases it is not possible to apply the Hori averaging method directly to obtain the solution (53), because ϖ is not circulating. Moreover, in certain cases it is observed that, for example, $|A| \simeq |B|$ and $C \simeq 0$, which implies that e can take values very close to zero. In such cases we have to deal with a singularity of the action-angle variables, because the angle ϖ is not defined at all!

Figure 7 shows the behavior of some real Trojans in the $(K, H) = \sqrt{-2W}(\cos\varpi, \sin\varpi)$ plane, as obtained from a numerical integration over several periods of Ω. We have used the RA15 integrator, and assumed Jupiter to be on a fixed elliptic inclined orbit, with $\varpi_1 = 11^\circ$. At first glance, we can see that all trajectories look roughly like circles, but some do not contain the origin. In the following pages, we show how to overcome the problems associated with these paradoxal librations.

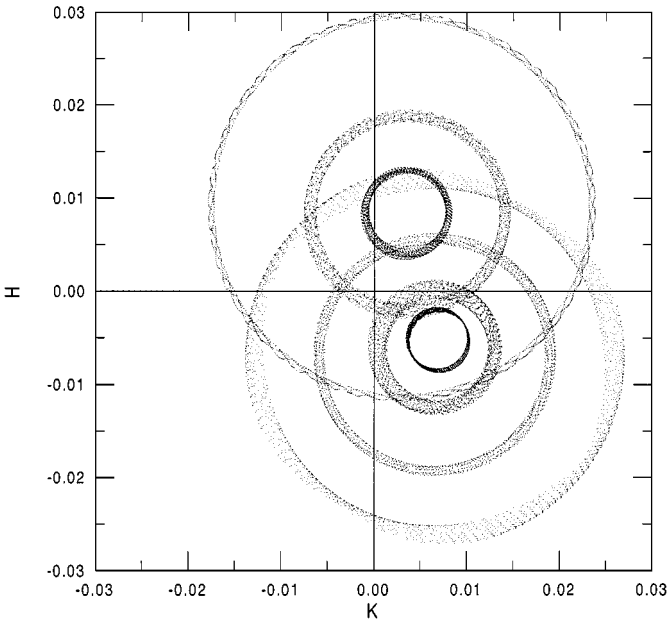

FIG. 7. Examples of the behavior in the plane $(K, H) = \sqrt{-2W}(\cos\varpi, \sin\varpi)$, showing some paradoxal librations. Orbits centered at $H > 0$ correspond to L_4, while orbits centered at $H < 0$ correspond to L_5.

Looking at Fig. 7, it is interesting to note that the center of the trajectories varies from asteroid to asteroid. According to Morais (1999), the location of these centers mostly depends on the amplitude of libration of the associated trajectories. It goes from $\varpi = \varpi_1 + 60^\circ$ for zero-amplitude orbits in L_4 ($\varpi_1 - 60^\circ$ in L_5), to $\varpi \simeq \varpi_1$ for orbits near the separatrix. Another interesting property observed in Fig. 7 is that the centers of the paradoxal librations do not significantly change with the evolution of (T, Ω). Indeed, the variation of (T, Ω) causes a motion of the center which translates only into the loops of the corresponding trajectory. This means that, fixing the orbit of Jupiter, the center of each trajectory is more or less invariant. Of course, this is not the case when a variation in (e_1, η_1) and (ϖ_1, Ω_1) is introduced. While the first two are responsible for a radial shift of the center, the latter two cause an angular motion of the center (Érdi 1981, 1988).

The center can be determined as the fixed point of Hamiltonian (50) in the (K, H) space, assuming $(T, \Omega, e_1, \eta_1, \varpi_1, \Omega_1)$ are fixed at their initial values. Recall that Hamiltonian (50) also depends on the amplitude of libration through the average over σ which is embedded in the coefficients. Then, we introduce a transformation to new variables (V, ψ), which is a simple translation of the origin similar to that of Eq. (24):

$$\sqrt{-2V}(\cos\psi, \sin\psi) = (K - K_f,\ H - H_f). \qquad (56)$$

Here (K_f, H_f) is the center which depends upon $(T, \Omega, e_1, \eta_1, \varpi_1, \Omega_1)$. The next step is to reexpand Hamiltonian (50) in terms of the new set of variables (V, T, ψ, Ω). This does not render any significant loss of performance in our procedure, since the calculation of each expansion takes only a few seconds of CPU time. In this way we arrive at a Hamiltonian $\bar{F}(V, T, \psi, \Omega; e_1, \eta_1, \varpi_1, \Omega_1)$, where ψ is now a circulating angle, such that $\nu_\psi = \nu_\varpi$. Thus, this Hamiltonian can be solved following either of the two approaches described in Section 4.2.

It is worth noting that the transformation (56) has the additional advantage of removing the contribution K_f, H_f of the forced terms to the calculation of the proper elements. Thus, in our model, this transformation is always applied, even when no paradoxal libration exists.

4.3. Additional Perturbations

Until now we have considered a constant orbit of Jupiter, and all the previous calculations and comparisons have been performed in this scenario (with the exception of the proper elements shown in Figs. 6a,b). In the true Solar System, however, the orbit of the perturber suffers variations due to the perturbations of the remaining planets. A model for proper elements that pretends to be valid for long timescales must include these effects.

4.3.1. Secular perturbations of Jupiter. The secular variation of Jupiter's orbit translates fundamentally into the variation of four orbital elements: $(e_1, \eta_1, \varpi_1, \Omega_1)$. Their evolution with time is usually represented by a series of harmonics of the type

$$\begin{aligned} e_1 E^{\sqrt{-1}\varpi_1} &\equiv k_1 + \sqrt{-1}h_1 = \sum_{k=5}^{8} G_k E^{\sqrt{-1}(g_k t + \delta_k)} \\ \eta_1 E^{\sqrt{-1}\Omega_1} &\equiv p_1 + \sqrt{-1}q_1 = \sum_{k=5}^{8} S_k E^{\sqrt{-1}(s_k t + \varphi_k)}, \end{aligned} \qquad (57)$$

where g_k, s_k are the fundamental secular frequencies of the outer planets; δ_k, φ_k are phase angles (dependent on the initial conditions); and G_k, S_k are the amplitudes. In this work, the numerical values adopted for these parameters were taken from the synthetic planetary theory LONGSTOP 1B of Nobili *et al.* (1989). The initial phases of the theory (see Table 3 of that paper) correspond to the date JD 2440400.5.

Although the so-called great inequality of Jupiter's mean longitude is known to be very important in studying Saturn's hypothetical Trojans (De la Barre *et al.* 1996), in the case of Jupiter this perturbation can be neglected without any loss in precision.

Now, we have to introduce the secular solution (57) in our expansion of the Hamiltonian function (Eq. 50). First, we rewrite this latter expression as

$$\begin{aligned} &\bar{F}(W, T, \varpi, \Omega, t) \\ &\quad = \sum_{i,j,k,l} W^i T^j E^{\sqrt{-1}(k\varpi + l\Omega)} \times \sum_{m,n=0}^{3} \sum_{p,q=0}^{2} \tilde{A}_{i,j,k,l,m,n,p,q} \\ &\quad \times (k_1)^m (h_1)^n (p_1)^p (q_1)^q, \end{aligned} \qquad (58)$$

and from (57) we can determine the products and powers of Jupiter's elements as functions of the time. For arbitrary values of m, n, p, q, these are written as

$$(k_1)^m (h_1)^n (p_1)^p (q_1)^q = \sum_u C_{u,m,n,p,q} E^{\sqrt{-1}(u\cdot\phi t)}, \qquad (59)$$

where t is the time, $u = (u_1, u_2, \ldots, u_8)$ is a vector of integers, not all different from zero, $\phi = (g_5, g_6, g_7, g_8, s_5, s_6, s_7, s_8)$ is the vector containing all the fundamental frequencies, and $(\cdot)$ represents the scalar product. Notice in this expression that the phase angles δ_k, φ_k have all been embedded into the coefficients $C_{u,m,n,p,q}$. Introducing (59) into (58), and computing the new coefficients, we finally arrive at

$$\bar{F}(W, T, \varpi, \Omega, t) = \sum_{i,j,k,l} \sum_u D_{i,j,k,l,u} W^i T^j E^{\sqrt{-1}(k\varpi + l\Omega + u\cdot\phi t).} \qquad (60)$$

Since the resulting number of terms in (59) is enormous, in practice we only consider those harmonics whose contribution to (60) renders amplitudes $D_{i,j,k,l,u}$ larger than 10^{-7} the value of the largest amplitude in the Fourier spectrum determined by fast Fourier transform (FFT). This threshold is chosen so as to guarantee that not only the disturbing function but also its derivatives are well reproduced using this truncated expression.

Equation (60) constitutes our final expression of the three-body Hamiltonian describing the evolution over long timescales. It is worth noting that this Hamiltonian can be solved (once again) applying a first order Hori's averaging method. In this case, each argument $(u \cdot \phi t)$ is to be treated as a linear function of time, thus having a constant conjugate momentum $(u \cdot \phi)\, \Lambda_u$.

4.3.2. Direct perturbations of other planets. As a final improvement, we also include in our model the so-called *direct perturbations* of nonresonant planets. We take into account the direct gravitational effect of the three outermost jovian planets (Saturn, Uranus, and Neptune) on the asteroid. In order to simplify the calculations, we consider these planets to be moving on fixed circular orbits with zero inclination. The mean values of a and the masses are taken from the planetary theory of Bretagnon (1982). This circular–planar approach should be enough for our purposes, since the main effect of these direct perturbations is to slightly modify the location of fixed points and secular resonances inside the 1:1 resonance.

The averaged disturbing function of the direct perturbations, $R_{\rm D}$, is then computed as

$$R_{\rm D}(L, W, T, \varpi, \Omega) = \frac{\mu}{4\pi^2} \int_0^{2\pi} \int_0^{2\pi} \sum_{\rm p} m_{\rm p} \left(\frac{1}{\Delta_{\rm p}} - \frac{r \cos \Phi_{\rm p}}{r_{\rm p}^2} \right) d\lambda\, d\lambda_{\rm p}, \qquad (61)$$

where the subindex $\rm p = 2, 3, 4$ refers to the planet under consideration, and $\Delta_{\rm p}$ is the planet-asteroid distance. In practice, the determination of $R_{\rm D}$ is carried out using an asymmetric expansion analogous to that described in Section 3.3. The double averaging comes from the fact that the asteroid is not involved in a mean motion resonance with $m_{\rm p}$. As a consequence, the indirect part disappears, and the disturbing function does not depend on the resonant angle $\sigma = \lambda - \lambda_1$. Then, its contribution to the motion of the Trojans on short timescales (i.e., to Eq. 47) translates only into a change of the libration period. This must be taken into account at the time of performing the average over the first degree of freedom, described in Section 4.2, to obtain $\bar{F}$ (Eq. 60). Note that the average over the first degree of freedom must also be extended to $R_{\rm D}$. Indeed, since $R_{\rm D}$ depends on L, it also depends on (J^*, θ^*) through relations similar to (49). After the average over the first degree of freedom, we end up with a new function $\bar{R}_{\rm D}(W, T, \varpi, \Omega)$, and the complete Hamiltonian for describing the motion of the Trojans over long timescales is given by the sum of $\bar{F}$ (from Eq. 60) and $\bar{R}_{\rm D}$.

5. THE PROPER ELEMENTS

We now have all the tools necessary to determine the proper elements of the Trojan asteroids. However, the application of our model requires that we start with a suitable set of *mean elements*, i.e., values of the orbital elements for which the short periodic variations (associated with the orbital periods of the perturbing bodies) have been removed. In principle, this can be done analytically by means of a series of canonical transformations (Knežević *et al.* 1988, Milani and Knežević 1999). However, we prefer to use a more direct and easier-to-implement numerical approach. This consists of a short numerical integration (over a few hundred years) applying a low-pass digital filter to the output, which efficiently removes all the high frequencies in the Fourier spectrum. It is worth recalling that filtered elements are not necessarily the same as mean elements, since an average in the time domain cannot be directly related to a convolution in the frequency domain. However, the experience shows that if the filter is efficient enough, the filtered elements constitute quite a good approximation of the mean ones (see, for example, Ferraz-Mello 1994).

We proceeded as follows. First, the osculating orbital elements of all the numbered and multiopposition Trojans were taken from the Asteroids Database of Lowell Observatory, as of December 2000. We assume an asteroid to be multiopposition if the orbital arc spanned by its observations is larger than 390 days. The total number of bodies was 533, of which 313[6] are located around $\rm L_4$, and 220 around $\rm L_5$.

The osculating elements at the initial epoch JD 2451900.5 were numerically propagated using the well known symplectic integrator SWIFT (Levison and Duncan 1994), and considering

[6] We have also included a body, *2000 XN9*, which has an arc of 360 days but appears as multiopposition in the List of Trojans maintained at the Harvard Center for Astrophysics (`http://cfa-www.harvard.edu/iau/lists/JupiterTrojans.html`).

a model of the Solar System which includes the four outer major planets. Initial conditions for the planets were taken from JPL Ephemerides DE405. The masses of the inner planets were added to the Sun, and the initial conditions of all bodies were recalculated to refer them to the barycenter of the inner Solar System. The adopted reference plane for the simulation was the invariable plane of the LONGSTOP1B theory (Nobili *et al.* 1989). The total simulation spanned 300 yr, with a time step of 10 days. We have incorporated in the integrator a set of procedures to perform an online digital filtering of the output. A finite impulse responce (FIR) filter in the time domain was applied to the variables $aE^{\sqrt{-1}\sigma}$, $eE^{\sqrt{-1}\varpi}$, and $\sin(I/2)E^{\sqrt{-1}\Omega}$ obtained in the integration. This filter is very similar to those designed by Carpino *et al.* (1987). It has symmetric normalized coefficients with a decimation factor of 50, and allows suppression of all periods between 0.7 and 35 yr, with a large attenuation factor ($<10^{-3}$). This effectively removed the short period oscillations related to the orbital motion of Jupiter and Saturn. The orbital periods of Uranus and Neptune cannot be removed without degrading the quality of the resulting mean a and σ, since they are of the same order of the period of libration. In this way, we ended up with a set of initial mean values $(L, W, T, \sigma, \varpi, \Omega)$ for each asteroid. We defined $t = 0$ as the initial time for which these mean values are given (in our case, JD 2499350.5) and aligned the initial phases of the secular theory (Eqs. 57) accordingly.

The next step involves the transformation to local variables $(J, W, T, \theta, \varpi, \Omega)$ at $t = 0$, the asymmetric expansion of the Hamiltonian, and the averaging over the first degree of freedom. Once again, it is worth recalling that the direct perturbations from Saturn to Neptune are already taken into account at this stage of the model. This results in a value of J^* (see Eq. 48) which is the first proper element, given as a function of the remaining degrees of freedom. In terms of the proper dynamical parameters introduced by Schubart and Bien (1987), the value of J^* is related to the amplitude of libration D. The first equation (48) determines how this amplitude varies as a function of the other variables of the system and of the initial conditions. In order to obtain a true invariant value of J^*, we will need to average this expression over these variables. We will see how to do this below.

Having relations (48) for J^* and θ^*, we obtain for each asteroid the long-term Hamiltonian $\bar{F} + \bar{R}_D$, which already includes the secular variation of Jupiter's orbit. As mentioned above, this Hamiltonian can be solved by using Hori's method. This involves the previous transformation $(W, T, \varpi, \Omega) \to (V, T, \psi, \Omega)$ to remove the forced eccentricity, and leads to the actions V^*, T^*, which constitute the second and third proper elements. However, care must be taken at this point for possible small divisors arising for asteroids that may be in the vicinity of secular resonances. These can be identified as harmonics in the Hamiltonian such that $k\nu_\varpi + l\nu_\Omega + u \cdot \phi \approx 0$, for some values of k, l, u. Particular cases are that of the Kozai resonance, corresponding to $k = -l$ and $u = 0$; and the ν_{16} resonance, corresponding to $k = 0, l = 1$, and $u \cdot \phi = -s_6$. It is important to point out that our method cannot detect the occurrence of such quasi-commensurabilites, except in the case where the small divisors are very close to zero, i.e., when the object is inside a secular resonance. Therefore, for quasi-commensurable asteroids, proper elements can still be estimated, although we expect that their precision will be degraded.

As a final step, we introduce the solution of the second and third degree of freedom, together with the secular variation of Jupiter's orbit, into the first equation (48). As we already mentioned, we proceed then to average J^* in order to eliminate its second order temporal variation and to obtain an invariant value, i.e.,

$$J^* = \frac{1}{\tau}\int_0^\tau J^*(J^0(t), \theta^0(t), V^*, T^*, \nu^*_\varpi t, \nu^*_\Omega t, u \cdot \phi t)\, dt, \quad (62)$$

where $\tau = 2\pi/\nu$ is such that $\nu = \min_u(\nu^*_\Omega, u \cdot \phi)$. It is worth noting that the initial conditions (J^0, θ^0) are not kept fixed during the average but varied in accordance to the variation of the other degrees of freedom.[7]

Since the set of proper elements (J^*, V^*, T^*) is cumbersome to interpret, we translate it to the better known set (D^*, e^*, I^*). This will furthermore facilitate comparisons with previous studies. The relation between J^* and D^* can be rather simply obtained from the inverse transformation to local variables (Eqs. 24–25). We fix L at its value at the libration point (K_c, H_c) and calculate the maximum and minimum values of σ, which correspond to the conditions $\theta = \pi/2$ and $3\pi/2$, respectively. For the remaining two elements, we adopted the definitions

$$\begin{aligned} e^* &= \left(1 - \frac{(V^* + L_c)^2}{L_c^2}\right)^{1/2} \\ I^* &= 2\arcsin\left(\frac{-T^*}{2(V^* + L_c)}\right)^{1/2}, \end{aligned} \quad (63)$$

where $L_c \approx \sqrt{\mu a_1}$. Note that, although the canonical proper elements V^*, T^* are related to the time averages of V, T, the same is not true for these definitions of e^* and I^*, since the average of the square root is not equal to the square root of the average.

This procedure was applied to our whole sample of 533 Trojans. The results in the planes (I^*, e^*) and (D^*, e^*) are shown in Fig. 8, where the populations for L_4 and L_5 are presented separately. We can see that both populations lie more or less within the same boundaries in each element. In particular, both distributions in the (D^*, e^*) plane lie below Rabe's stability curve (Rabe 1965, 1967), shown in dotted lines. Only two asteroids are found well above this limit: *(4835) 1989 BQ* in L_4 and *(5144) Achates* in L_5. Two other marginal cases are shown in Fig. 8b.

[7] When the other degrees of freedom are frozen, the trajectory in (J, θ) is a closed curve. But when they vary slowly, the trajectory is open. Thus, starting from an initial condition (J^0, θ^0), we arrive, after a period of θ, to another "initial" condition different from the original one.

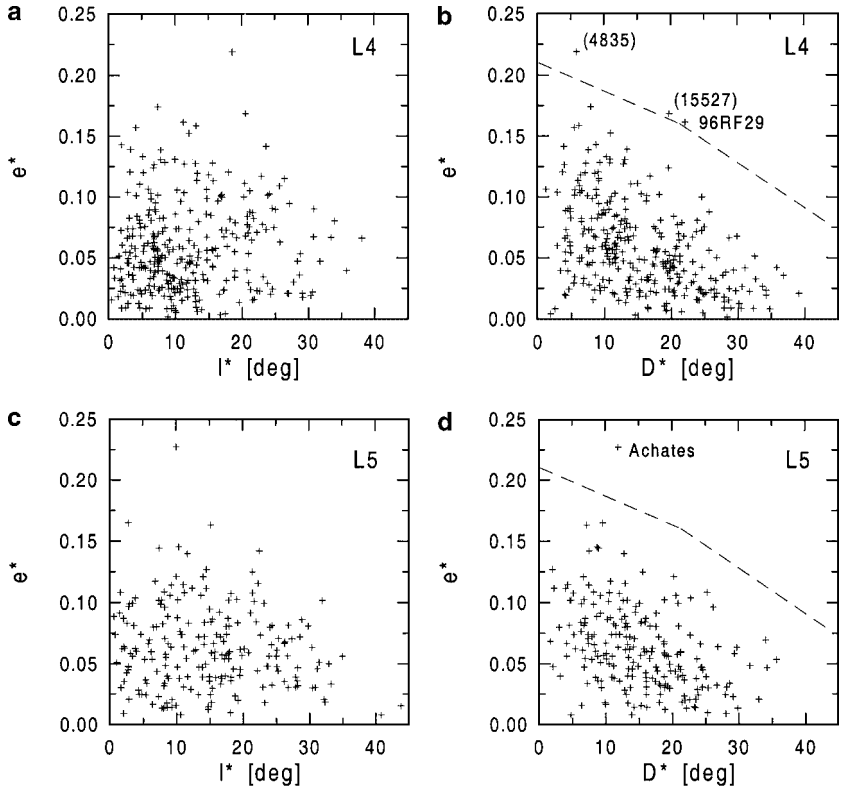

FIG. 8. Proper elements for L_4 and L_5 Trojans, as seen in the (e^*, I^*) plane and the (e^*, D^*) plane. The dashed line in (b) and (d) corresponds to Rabe's (1965) stability limit.

Nevertheless, we also note certain differences between the Lagrange points. The most conspicuous is an apparent cluster of bodies in Fig. 8a corresponding to low values of both elements, i.e., $(I^*, e^*) \sim (8^\circ, 0.05)$. In the case of L_5, such clustering is not observed.

5.1. *Accuracy and Stability*

The stability of our proper elements was determined by analyzing their variation over a long interval of time and computing their standard deviations. We did not perform this test for all the Trojans in our sample, but only for 20 of them chosen at random. These were numerically integrated over 5×10^7 yr, including perturbations from Jupiter to Neptune, and proper elements were calculated every 500,000 yr applying the procedure described above. From the analysis of the time variation of (D^*, e^*, I^*) for these 20 Trojans, we found typical values of the root mean square (r.m.s.) error of the order of 0.3°–0.4° in D^* and 0.003–0.004 in e^* and sin I^*. An example is shown in Fig. 9. The crosses represent the evolution of mean (filtered) elements of asteroid *(1873) Agenor*, located in the vicinity of L_5, as obtained from numerical integration using SWIFT. The thick horizontal lines correspond to the proper elements as determined from our model, adding the appropriate correction due to the forced eccentricity (i.e., we are plotting W^*, not V^*). The r.m.s is below 0.1%. On both plots we can see a very good agreement between our proper elements and what we expect to be the "average values" of the mean elements. In the case of W^* this agreement is about 0.05%. It degrades to 0.2% for T^*, where the proper element slightly overestimates the average of the mean element. This means that the estimated proper inclination results are slightly smaller than expected, which could be related to some forced term we are not taking into account in our model.

As a further check of the precision, we compared our results for the first 41 numbered Trojans with two data sets: Bien and Schubart (1987) and Milani (1993). The results are presented in Fig. 10 in the form of three plots. Each plot shows the proper elements determined by Bien and Schubart (1987) (crosses) and those determined in this paper (gray circles) the quantities estimated by Milani (1993; on the abscissa). As a reference, we also plotted a 45° line, which corresponds to the ideal case where all determinations coincide. We can see that, in the case of e^*, I^*, there is practically no difference between all three sets of values. The same is not observed, however, in the case of the amplitude of libration D^*. Although the precision is very good for small values of D^*, we note an increasing deviation of our proper element for large amplitudes. This deviation proved to be systematic and related to the early truncation of the asymmetric expansion of the disturbing function.

From the 533 members of our sample, our semianalytic method was unable to manipulate 19 asteroids, and proper elements could not be determined for them. We did a further

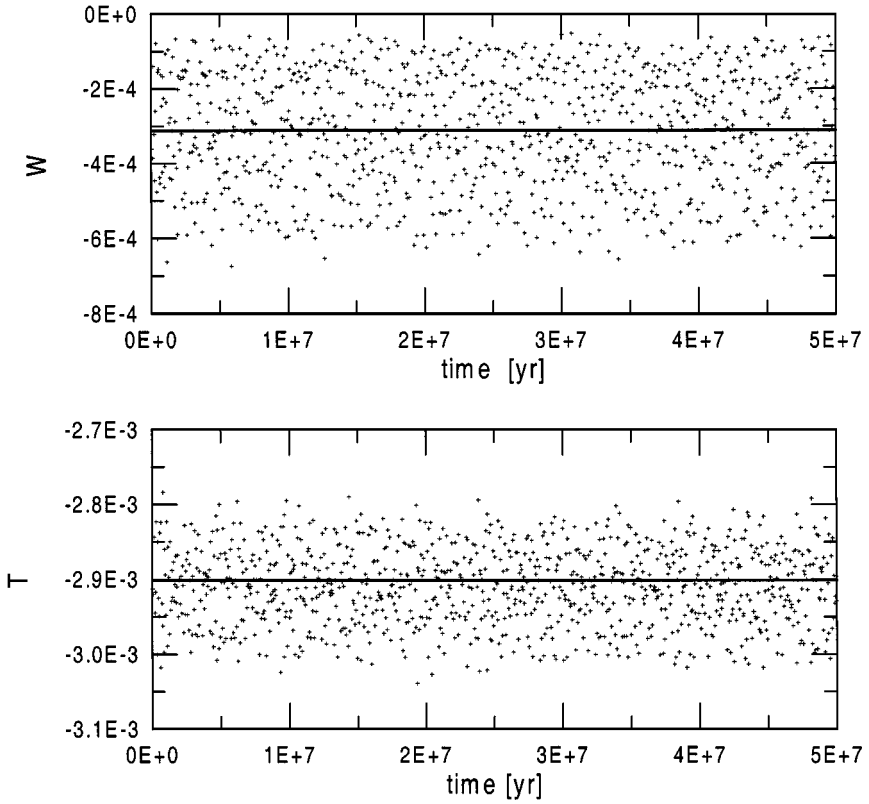

FIG. 9. Evolution of *(1873) Agenor* over 50 million years. Crosses are filtered elements from a numerical integration. Thick lines are the proper elements as calculated with our model. The r.m.s. is smaller than 0.1%.

analysis of these objects via direct numerical simulations using SWIFT. The simulations spanned 200,000 yr in the framework of a full N-body model, including perturbations of the four major planets. This analysis showed that the reasons our method failed in these cases can be divided into three distinct groups: (i) Two asteroids, *1997 SG14* and *2000 HR24*, are not located in tadpole orbits at all, but move in horseshoe-type trajectories. This is contrary to our original hypothesis for the motion of the Trojans, and the transformation to local variables is not defined in such a case. These two bodies suffered a close encounter with Jupiter in less than 10,000 yr and were ejected from the system. Basically, they are asteroids wrongly identified as Trojans. (ii) Ten asteroids, for example, *1998 WA15* and *(9807) 1997 SJ4*, were found in highly peculiar orbits, which do not even present similar periods of oscillation in inclination and longitude of node. Some of them appeared to be very close or inside the ν_{16} secular resonance. (iii) Seven bodies presented correlations between the frequencies of oscillation of the longitude of perihelion and the longitude of node. Of these, probably the most interesting case is *(15436) 1998 VU30*, which seems to exhibit a very-long-period behavior of the angle $\varpi + \Omega$ (see Fig. 11). Although this combination is probably not associated with any resonance, the resulting coupling between the slow degrees of freedom causes the nonconvergence of the averaging method (Section 4.2.2).

We did not find any other type of linear secular resonance which could affect the convergence of Hori's method during the resolution of the second and third degrees of freedom. In fact, according to Morais (2001), Jupiter's Trojans could only be affected by linear secular resonances involving Ω, mainly ν_{16}. Linear secular resonances involving the perihelion are almost absent, as well as the Kozai resonance which never holds. The effect of the secular resonances of the node translates into forced inclinations which are an order of magnitude smaller (in mass ratio) than the forced inclination due to Jupiter (which is already very small). This means that, even if a real Trojan is close to the ν_{16} resonance, for example, the net effect of this resonance on the value of the corresponding proper element should be negligible.

As a final comment, we must note that since we are working with a semianalytical integrable model, it is impossible for us to detect any chaos in the Trojan population with a single determination of proper elements. The values we determine are supposed to represent integrals of motion (i.e., values constant for all time), which, of course, is not true if the orbits are chaotic. This is an undesirable but inevitable approximation of the method. It is important to bear this in mind, especially during the search for asteroidal families, as discussed in the following section.

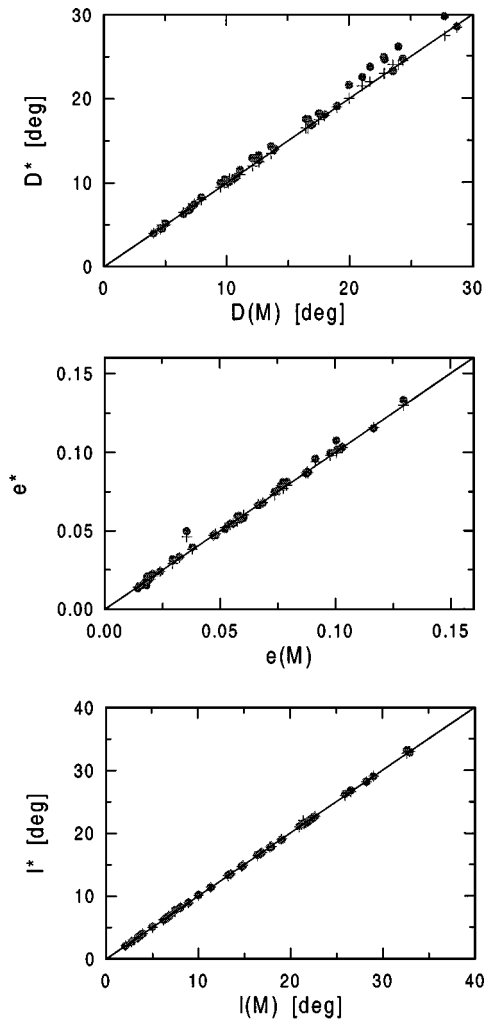

FIG. 10. Proper elements due to Bien and Schubart (1987) (crosses) and the values of this paper (gray circles), plotted with respect to the determinations of Milani (1993) (in the abscissas). Plots show only the first 41 numbered Trojans, which correspond to those computed by Bien and Schubart (1987).

6. ASTEROID FAMILIES IN THE TROJAN BELT

After calculating the proper elements, the next step was to try to identify clusters in the phase space of the momenta that may be associated with asteroid families in each libration region. Although the literature contains many works regarding asteroid families in the main asteroid belt (beginning with the pioneering work of Hirayama (1918), there is very little in the case of the Trojan belt. The three principal references are due to Bien and Schubart (1987), Shoemaker *et al.* (1989), and Milani (1993). Of these, only the latter work considered a sufficiently large number of bodies (174) so as to make the identification of families even marginally reliable. For this reason, all our comparisons will be done with this study.

Asteroid families are relics of the fragmentation of a large parent asteroid that occurred some time in the past. At present we can identify their members as clusters in the space of proper elements, which can be either orbital proper elements (D^*, e^*, I^*) or canonical actions (J^*, V^*, T^*). These agglomerations must be sufficiently compact so as to be statistically significant and well differentiated from the background population. In addition to this dynamical condition, candidates for families must also have chemical constitutions compatible with a common origin, since they are supposedly fragments of a single parent body. Unfortunately, all known Trojan asteroids show similar spectral signatures and they are mostly cataloged as D-type objects (Tholen 1989). Thus, family identification becomes possible only through dynamical considerations.

In order to study clusters in the space of proper elements, we first need to specify a "distance" or metric between any two points in this space. As Milani (1993) pointed out, the metrics d_1 and d_2 normally used in the case of main belt asteroids (Zappalà *et al.* 1990, 1994) are not directly applicable in the case of Trojans. Since we want to compare our results with those of Milani (1993), we adopt his d_3 metric, which can be written as

$$d_3 = \left[\frac{1}{4}\left(\kappa\frac{\delta D^*}{a_c}\right)^2 + 2(\delta e^*)^2 + 2(\delta \sin I^*)^2\right]^{1/2} \qquad (64)$$

where $\delta D^* = D_i^* - D_j^*$ is the difference between the proper libration amplitudes of bodies i and j. Similar definitions hold for δe^* and $\delta \sin I^*$. In this expression, $a_c = L_c^2/\mu$, and κ is a proportionality factor that relates D (in radians) with the amplitude of the oscillation in a (in AU). Following Érdi (1981, 1988), it can be expressed as

$$\kappa = \sqrt{3\frac{m_1}{1+m_1}}a_1 + \mathcal{O}(m_1) \simeq 0.278309. \qquad (65)$$

Considering that our method yields canonical elements, we could transform this metric into an equivalent expression in the (J^*, V^*, T^*) space. However, since we are going to compare orbits with very similar values of the elements, we prefer to use Eqs. (63)–(65) and work directly with d_3 without introducing any significant loss of precision.

After calculating the mutual distances between all bodies in the proper element space, we applied the well known hierarchical clustering method (HCM) (Zappalà *et al.* 1990). In this method, the distances between all Trojan couples (corresponding to the same Lagrange point) are sorted in ascending order. Then, for each value of the cutoff Q, the couples with $d_3 < Q$ are "clustered" together and the whole procedure is repeated again. The results of this process are usually presented in the form of dendrograms or "stalactite" diagrams for different values of the cutoff. The cutoff threshold at which the nominal family memberships are defined was taken to be $Q = 0.010$ in accordance with Milani (1993). This corresponds to relative velocities of the order of $\sim$130 ms^{-1}. It is worth noting that lower values of this threshold would be meaningless, since they are of the same order as the accuracy of our proper elements.

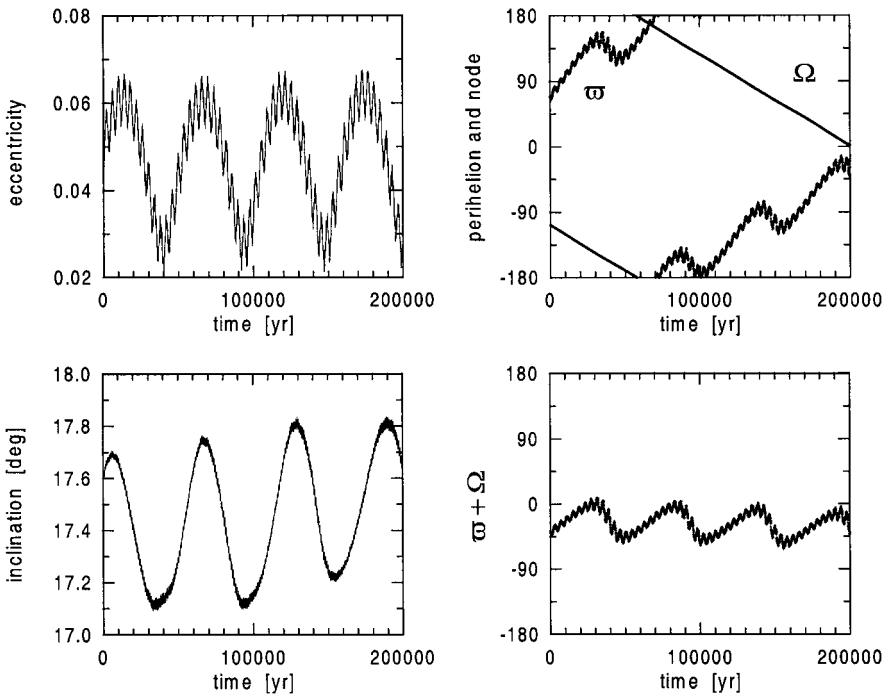

FIG. 11. Numerical simulation over 200,000 yr of *(15436) 1998 VU30*, showing the coupling between perihelion and node.

Finally, we need to specify the minimum number of members $N_{\min}$, at a given Q, for a cluster to be considered significant, i.e., to constitute a nominal family. According to Zappalà *et al.* (1995) this can be defined as $N_{\min} = N_0 + 2\sqrt{N_0}$, where N_0 is the average number of background bodies, obtained by subtracting the families that fall within a sphere of radius Q in the metric space. In our case, we adopt a slightly different definition for N_0. We consider a sphere of radius Q and center it on the i-th asteroid, counting the number of bodies falling inside the sphere, namely N_i. We repeat this procedure for every asteroid at a given Lagrange point, and define N_0 as the average value of N_i. Consequently, the resulting value of $N_{\min}$ will be a function not only of the cutoff but also of the total number of bodies in each swarm. In particular, for $Q = 0.010$, we obtained $N_{\min} = 5$ for the leading Trojans and $N_{\min} = 4$ for the trailing swarm. Then, we consider a cluster to constitute a statistically significant nominal family whenever its number of members N is greater than $N_{\min}$ (i.e., $N = 6$ or 5, respectively).

The results of this study are presented in Fig. 12. The nominal families appear in each case as tips of the stalactites for cutoffs below 0.01. We note significant differences between the Lagrange points. The L_4 region (Fig. 12a) shows four main families: *(1647) Menelaus* (24 members), *(2148) Epeios* (19 members), *(4035) 1986 WD* (6 members), and *(12917) 1998 TG16* (7 members). A fifth family, *(14690) 2000 AR25*, also appears in the dendrogram, although its population decreases below $N_{\min}$ at precisely the threshold value of the cutoff. The distribution of the members of each family in the space of proper elements e^*, I^* is shown in Fig. 13. Background objects are shown as small crosses while family members are plotted as filled circles. Note that family *(4035)* appears more like a chain identification (which is a well known drawback of the HCM) than like a cluster. We can see that all families lie in the low-eccentricity region and have moderate inclinations. Comparing this plot with Fig. 8,

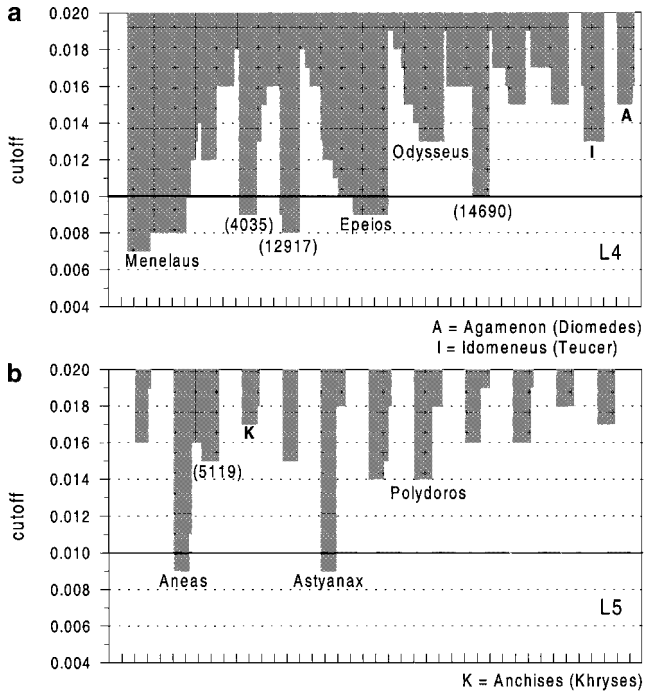

FIG. 12. Dendrograms for both L_4 and L_5 libration regions. At each value of the cutoff, the width of the stalactites represents the number of bodies in each family. One tick in the abscissas = 5 bodies.

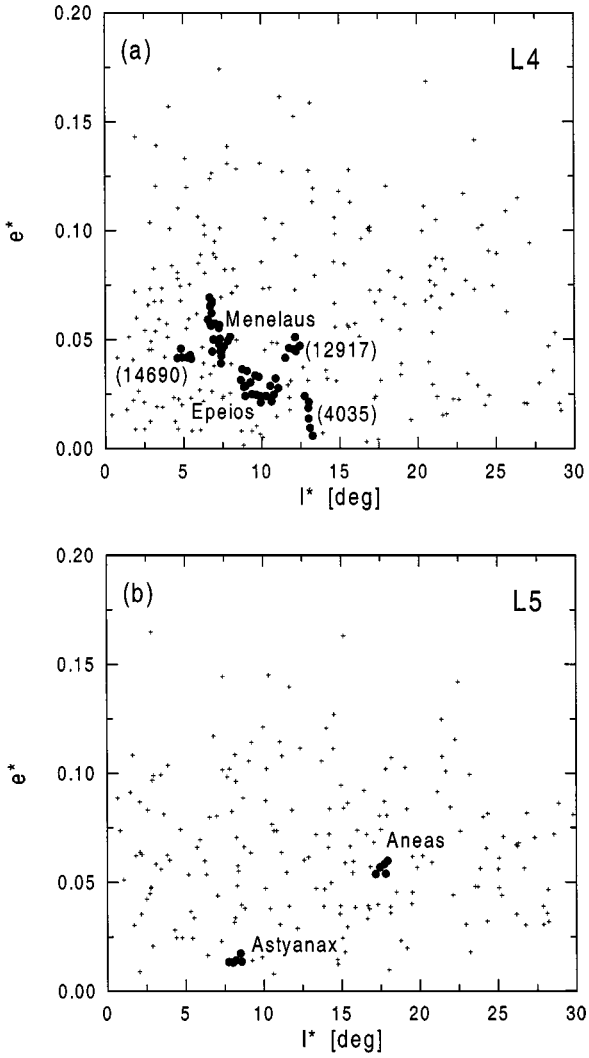

FIG. 13. Asteroidal families in L_4 and L_5 (filled circles). Background Trojans are represented by small crosses. Note that family *(4035)* appears in L_4 more as a "chain" than as a cluster.

we note that these candidates for asteroid families coincide precisely with the clusters observed in the low-eccentricity region of this swarm.

Results for the population in the L_5 region are shown in Fig. 12b. Here we see a different story. Even considering a lower value of $N_{\min}$ in order to compensate for the smaller amount of data, we find much less statistically significant agglomerations at $Q = 0.01$. Only two clusters appear at this cutoff: *(1172) Aneas* and *(1871) Astyanax* each with 5 members, which is precisely the minimum number of bodies per family for this swarm.

Although members of the same family are well clustered regarding their proper eccentricities and inclinations (Fig. 13), the same is not true for the proper amplitude of libration. The values of D^* for all the members of the same family, both in L_4 and L_5, are always rather spread. However, it is interesting to note that, in all the families detected, the proper amplitudes distribute more or less in the same interval, which goes from about 5–10° to 25–30°.

A comparison between these results and those of Milani (1993) shows agreements and differences. These are summarized in Table I (for a cutoff of 0.016) and Table II (for a cutoff of 0.010). The number at the right of each family name denotes the number of members at that value of Q. The first two columns correspond to L_4, while the other two pertain to L_5. In Table I, we see very good agreement between the two works, as far as the leading Trojans are concerned. Of the five families mentioned by Milani (1993), four were identified in our sample, and only *(2456) Palamedes* is missing in our calculation and is probably a statistical fluke. Note that *(2759) Idomeneus* and *(911) Agamenon* were formerly identified as *(2797) Teucer* and *(1437) Diomedes*, respectively. Conversely, we detect six other agglomerations not previously found. Of these, *(2148) Epeios* is the largest, containing a total of 30 members. The absence of these clusters in Milani's work seems, at first glance, to be strange since their size is at least comparable with the previously detected families. Nevertheless, analyzing their members, we note that almost all of them were not known in the year 1993. For the trailing Trojans, the agreement is similar. Both studies identify *(4708) Polydoros* and *(5119) 1988 RA1*, but not the remaining agglomerations. Once again, this is partly due to the different data sets used in the two studies, but also to the different values of $N_{\min}$. In Milani's (1993) study, this value was taken as equal to 2. Thus, unless one of these clusters has increased in size, they would not be detected in our analysis. This is precisely the case for *(4707) Khryses*, which we identified at $Q = 0.017$ as *(1173) Anchises*, with 5 members, and which disappears for lower cutoffs.

Comparisons in Table II show similar results. *Menelaus* once again appears in both studies and, especially in our case, still retains a very large membership. This cluster is probably the most robust candidate for a "real" Trojan family whose members share a common physical origin. *Epeios* also appears in our sample, and still maintains a respectable size. The remaining groups in L_4 show a significant decrease of members. Several disappeared from our column since their membership diminished below $N_{\min}$. *(4035) 1986 WD* breaks up, and a splinter family, *(12917) 1998 TG16*, appears around $Q = 0.015$, although their individual populations are very close to the minimum. In the case of L_5, only two families with at least five members survive in our calculation, both with the minimum number of members. Milani's (1993) *(2223) Sarpedon* only contained four members at $Q = 0.016$, and completely disappeared at this cutoff. Only *(1172) Aneas* and *(1871) Astyanax* survived, with populations practically undiminished with respect to Table I.

We must note that the difference observed in the results may be caused by the adopted values of $N_{\min}$ in each case, and consequently some of these families could just be statistical flukes. However, we must note that our proper elements are not as precise as those determined by Milani (1993), and this may part of the reason for the discrepancy.

TABLE I
Families Detected in Our Study for a Cutoff of 0.016, and Comparison with Milani's (1993) Families

L_4		L_5	
Milani (1993)	This work	Milani (1993)	This work
Menelaus (8)	Menelaus (41)	Polydoros (3)	Polydoros (6)
Teucer (6)	Idomeneus (9)	(5119) 1988RA1 (3)	(5119) 1988RA1 (11)
Diomedes (3)	Agamenon (7)	Sarpedon (3)	—
(4035) 1986WD (3)	(4035) 1986WD (22)	Kryses (3)	—
Palamedes (3)	—	—	Helenos (7)
—	Epeios (30)	—	Aneas (6)
—	Odysseus (15)	—	Phereclos (6)
—	(14690) 2000AR25 (9)	—	Deiphobus (5)
—	Euneus (7)	—	Astyanax (5)
—	Eurymedon (6)	—	Cloanthus (5)
—	(9590) 1991DK1 (6)	—	(11887) 1990TV12 (5)

Note. The two leftmost columns correspond to L_4 and the other two to L_5. The number in brackets at the right of each family name is the corresponding number of members.

7. CONCLUSIONS

In this work we have developed a semianalytical model for the motion of Trojan asteroids over long timescales. The present method is characterized by three main features:

- The transformation of the resonant angle to local variables. This geometrical approach allows us to avoid the usual problems associated with the calculation of action-angle variables in a resonant case, and to define a new set of canonical variables in which all the angular variables circulate.
- The application of the theory of adiabatic invariance, that allowed us to treat each degree of freedom separately. This was possible due to the different timescales associated with the temporal variation of each degree of freedom, and this is a characteristic of the Trojan dynamics.
- The use of an asymmetric Taylor–Fourier analytic expansion of the disturbing function, allowing us to perform all calculations in an explicit way.

We must note, however, that our approach cannot be considered as a perturbation theory "strictu sensu," but rather as a set of tools which simplifies the application of classical (nonresonant) perturbation theories, such as Hori's method.

With this model, we were able to estimate proper elements for almost the entire current population of Trojans with well determined orbits. The errors associated with these proper elements are typically about twice the errors obtained with previous numerical studies. However, the main advantage of our model lies in the fact that it is semianalytic in nature. On one hand, this means the model is "universal" and is not restricted to the jovian system or to the present population of asteroids. On the other hand, it is much faster than a numerical simulation. For example, the calculation of the proper elements for each asteroid takes about 2 min of CPU time on a Pentium III at 800 MHz. The analysis of the complete Trojan swarm took a little over one day. In comparison, the numerical integration of the same system for 10^7 yr with the SWIFT code, without any spectral analysis or additional calculations, is about 30 times slower and requires huge storage capacity.

Results of our search for asteroidal families has yielded several agglomerations in the L_4 swarm. Of these, *Menelaus* appears as the most robust and probable candidate for a real family of physically related objects. The size distribution of its members shows only two asteroids with diameters of the order of 80 km (*(1647) Menelaus* and *(1749) Telamon*), three bodies in the 40–50 km range, plus a large number of bodies with sizes of the order of 20–30 km.[8] Simulations on the collisional evolution of Trojans by Marzari *et al.* (1997) showed that such a family could be the natural by-product of the breakup of a parent asteroid of the size of the order of 200 km during the age of the Solar System. Similar considerations hold in the case of the *1986 WD*, whose largest members have sizes of the order of

TABLE II
Families Detected in Our Study for a Cutoff of 0.010, and Comparison with Milani's (1993) Families

L_4		L_5	
Milani	This work	Milani	This work
Menelaus (4)	Menelaus (24)	Sarpedon (3)	—
Teucer (4)	—	—	Aneas (5)
—	Epeios (19)	—	Astyanax (5)
—	(12917) 1998TG16 (7)	—	—
—	(4035) 1986WD (6)	—	—
—	(14690) 2000AR25 (6)	—	—

[8] When the IRAS diameter of the body is unknown, we have estimated it assuming a mean albedo of 0.04.

60 and 80 km. On the other hand, the family of *Epeios* does not fall into this category since all its members have diameters less than 40 km. It is interesting to compare these results with Milani's (1993) *Teucer* family. Its two largest members (*(2797) Teucer* and *(2759) Idomeneus*) have sizes of 119 and 68 km, respectively, which are at least in the same range as the biggest members of *Menelaus*. However, if this cluster were a real family, we would expect a very large number of small bodies (in the 20–40 km range) accompanying the agglomeration, and we have found no sign of these bodies. This property, together with the fact that we detected the agglomeration only for large values of the cutoff, makes us doubtful about the existence of this family. Similar results are also found in the case of Milani's (1993) *Diomedes* family, which has very few objects, all of them very large. As a final note, we recall that all our detected agglomerations lie more or less in the same region of the proper element's space. So we cannot rule out the possibility that all of them are members of a bigger "clan" (as is the case with *Flora*'s family in the asteroid belt), which would only become noticeable with an increasing number of observed bodies.

The clusters detected in L_5 are much less significant than those in L_4, even allowing for the difference in the base population. Although we found two agglomerations at low values of the cutoff, their number of members is very small. Their size distribution is similar to that of *Teucer* and *Diomedes*; i.e., one large body with diameter of the order of 100 km, and few very small companions. Nevertheless, they form very compact clusters which keep their numbers of members constant for almost all values of the cutoff. Their dispersion in the space of proper e and I is also much smaller than the families in L_4, as can be appreciated from Fig. 13.

On a final note, the present study was intended to improve on previous knowledge concerning the existence of families among Trojan asteroids. Nevertheless, it is difficult to say whether or not the observed differences between L_4 and L_5 are related to the collisional history of each swarm, their individual dynamical evolution, cosmogonic processes, or even observational bias. We hope further studies of the dynamics of the jovian Lagrange regions, together with improved observational knowledge of the Trojan population, will shed new light on this question.

The database containing our proper elements is available upon request.

ACKNOWLEDGMENTS

This work began during a visit of C. Beaugé to the Institute of Astronomy and Geophysics of the University of São Paulo (Brazil). The São Paulo State Science Foundation (FAPESP) is greatly acknowledged for funding that visit and this work. We also thank S. Ferraz-Mello for many valuable discussions and recommendations about this work. The detailed reviews of Z. Knežević and M. H. Morais, and the challenging comments of A. Morbidelli, helped to improve the manuscript and are greatly appreciated. Finally, we thank M. Vermes for carefully revising the manuscript and fixing several grammatical errors.

REFERENCES

Bien, R., and J. Schubart 1983. Long periods in the three-dimensional motion of Trojan asteroids. In *Dynamical Trapping and Evolution in the Solar System* (V. V. Markellos and Y. Kozai, Eds.), pp. 153–161. D. Reidel Dordrecht.

Bien, R., and J. Schubart 1987. Three characteristic orbital parameters for the Trojan group of asteroids. *Astron. Astrophys*. **175**, 292–298.

Bretagnon, P. 1982. Théorie du mouvement de l'ensemble des planètes. Solution VSOP82. *Astron. Astrophys*. **114**, 278–288.

Burger, Ch., E. Pilat-Lohinger, R. Dvorak, and A. Christaki 1998. Proper elements and stability of the Trojan asteroids. In *Impact of Modern Dynamics in Astronomy* (J. Henrard and S. Ferraz-Mello, Eds.), Kluwer Academic, Dordrecht.

Carpino, M., A. Milani, and A. M. Nobili 1987. Long-term numerical integrations and synthetic theories for the motion of the outer planets. *Astron. Astrophys.* **181**, 182–194.

De la Barre, C. M., W. M. Kaula, and F. Varadi 1996. A study of orbits near Saturn's triangular Lagrangian points. *Icarus* **121**, 88–113.

Érdi, B. 1981. The perturbations of the orbital elements of Trojan asteroids. *Celest. Mech.* **24**, 377–390.

Érdi, B. 1988. Long period perturbations of Trojan asteroids. *Celest. Mech.* **43**, 303–308.

Everhart, E. 1985. An efficient integrator that uses Gauss-Radau spacings. In *IAU Colloquium 83. Dynamics of Comets: Their Origin and Evolution* (A. Carusi and G. Valsecchi, Eds.), pp. 185. Reidel, Dordrecht.

Ferraz-Mello, S. 1994. Dynamics of the asteroidal 2/1 resonance. *Astron. J.* **108**, 2330–2337.

Ferraz-Mello, S., and M. Sato 1989. The very-high-eccentricity asymmetric expansion of the disturbing function near resonances of any order. *Astron. Astrophys.* **225**, 541–547.

Giorgilli, A., and C. Skokos 1997. On the stability of the Trojan asteroids. *Astron. Astrophys.* **317**, 254–261.

Henrard, J. 1970. *Perturbation Technique in the Theory of Nonlinear Oscillations and in Celestial Mechanics*. Boeing Scientific, Research, Laboratory, Technical, Note 051.

Henrard, J. 1990. A Seminumerical perturbation method for separable Hamiltonian systems. *Celest. Mech. Dynam. Astron.* **49**, 43–67.

Henrard, J. 1993. The adiabatic invariant in classical mechanics. In *Dynamics Reported*, pp. 197–218. Springer-Verlag, Berlin/New York.

Henrard, J., and J. Roels, 1974. Equivalence for lie transforms. *Celest. Mech.* **10**, 497–512.

Hirayama, K. 1918. Groups of asteroids probably of common origin. *Astron. J.* **31**, 185–188.

Jupp, A. H. 1969. A solution of the ideal resonance problem for the case of libration. *Astron. J.* **74**, 35–43.

Jupp, A. H. 1970. On the ideal resonance problem. *Mon. Not. R. Astron. Soc.* **148**, 197–210.

Knežević, Z., M. Carpino, P. Farinella, Ch. Froeschlé, C. Froeschlé, R. Gonczi, B. Jovanović, P. Paolicchi, and V. Zappalà 1988. Asteroid short-periodic perturbations and the accuracy of mean orbital elements. *Astron. Astrophys.* **192**, 360–369.

Knežević, Z. 1994. Asteroid proper elements: Past and present. In *Seventy-Five Years of Hirayama Asteroid Families: The Role of Collisions in the Solar System History* (Y. Kozai, R. P. Binzel, and T. Hirayama, Eds.), pp. 129–139. ASP Conf. Ser. **63**.

Knežević, Z., Ch. Froeschlé, A. Lemaítre, A. Milani, and A. Morbidelli 1995. Comparison between two theories of asteroid proper elements. *Astron. Astrophys.* **293**, 605–612.

Knežević, Z., and A. Milani 2001. Synthetic proper elements for the outer main belt asteroids. *Celest. Mech. Dynam. Astron.* in press.

Lemaître, A. 1993. Proper elements: What are they? *Celest. Mech. Dynam. Astron.* **56**, 103–119.

Lemaître, A., and A. Morbidelli 1994. Proper elements for highly inclined asteroidal orbits. *Celest. Mech. Dynam. Astron.* **60**, 29–56.

Levison, H. F., E. M. Shoemaker, and C. S. Shoemaker 1997. Dynamical evolution of Jupiter's Trojan asteroids. *Nature* **385**, 42–44.

Levison, H. F., and M. J. Duncan 1994. The long-term dynamical behavior of short-period comets. *Icarus* **108**, 18–36.

Marzari, F., P. Farinella, D. R. Davis, H. Scholl, and A. Campo Bagatin 1997. Collisional evolution of Trojan asteroids. *Icarus* **125**, 39–49.

Marzari, F., and H. Scholl 2000. The role of secular resonances in the history of Trojans. *Icarus* **146**, 232–239.

Milani, A. 1993. The Trojan asteroid belt: Proper elements, stability, chaos and families. *Celest. Mech. Dynam. Astron.* **57**, 59–94.

Milani, A., and Z. Knežević 1990. Secular perturbation theory and computation of asteroid proper elements. *Celest. Mech. Dynam. Astron.* **49**, 347–411.

Milani, A., and Z. Knežević 1994. Asteroid proper elements and the dynamical structure of the asteroid main belt. *Icarus* **107**, 219–254.

Milani, A., and Z. Knežević 1999. Asteroid mean elements: Higher order and iterative theories. *Celest. Mech. Dynam. Astron.* **71**, 55–78.

Morais, M. H. 1999. A secular theory for Trojan-type motion. *Astron. Astrophys.* **350**, 318–326.

Morais, M. H. 2001. Hamiltonian formulation of the secular theory for Trojan-type motion. *Astron. Astrophys.* **369**, 677–689.

Morbidelli, A., and M. Moons 1993. Secular resonances inside mean motion commensurabilities: The 2/1 and 3/2 cases. *Icarus* **102**, 316–332.

Morbidelli, A., and M. Moons 1995. Secular resonances inside mean motion commensurabilities: The 4/1, 3/1, 5/2, and 7/3 cases. *Icarus* **114**, 33–50.

Namouni, F., and C. D. Murray 2000. The effect of eccentricity and inclination on the motion near the Lagrangian points L4 and L5. *Celest. Mech. Dynam. Astron.* **76**, 131–138.

Nobili, A. M., A. Milani, and M. Carpino 1989. Fundamental frequencies and small divisors in the orbits of the outer planets. *Astron. Astrophys.* **210**, 313–336.

Pilat-Lohinger, E., R. Dvorak, and Ch. Burger 1999. Trojans in stable chaotic motion. *Celest. Mech. Dynam. Astron.* **73**, 117–126.

Rabe, E. 1965. Limiting eccentricities for stable Trojan librations. *Astron. J.* **70**, 687–688.

Rabe, E. 1967. Third-order stability of the long-period Trojan librations. *Astron. J.* **72**, 10–17.

Roig, F., A. Simula, S. Ferraz-Mello, and M. Tsuchida 1998. The high-eccentricity asymmetric expansion of the disturbing function for nonplanar resonant problems. *Astron. Astrophys.* **329**, 339–349.

Shoemaker, E. M., C. S. Shoemaker, and R. F. Wolfe 1989. Trojan asteroids: Populations, dynamical structure and origin of the L_4 and L_5 swarms. In *Asteroids II* (R. P. Binzel, T. Gehrels, and M. S. Matthews, Eds.), pp. 487–523. Univ. of Arizona Press, Tucson.

Schubart, J., and R. Bien 1987. Trojan asteroids: Relations between dynamical parameters. *Astron. Astrophys.* **175**, 299–302.

Tholen, D. J. 1989. Asteroid taxonomic classifications. In *Asteroids II* (R. P. Binzel, T. Gehrels, and M. S. Matthews, Eds.), pp. 1139–1150. Univ. of Arizona Press, Tucson.

Williams, J. G. 1969. *Secular Perturbations in the Solar System.* Ph.D. thesis, U.C.L.A., Los Angeles.

Woltjer, J. Jr. 1924. Critical terms associated with the libration in the theory of the Trojans. *Bull. Astron. Inst. Netherlands* **II**, 37–46.

Zappalà, V., A. Cellino, P. Farinella, and Z. Knežević 1990. Asteroid families I: Identification by hierarchical clustering and reliability assessment. *Astron. J.* **100**, 2030–2046.

Zappalà, V., A. Cellino, P. Farinella, and A. Milani 1994. Asteroid families II: Extension to unnumbered multi opposition asteroids. *Astron. J.* **107**, 772–801.

Zappalà, V., Ph. Bedjoya, A. Cellino, P. Farinella, and C. Froeschlé 1995. Asteroid families: Search of a 12,487-asteroid sample using two different clustering techniques. *Icarus* **116**, 291–314.

Anexo:

Planetary migration and the effects of mean motion resonances in Jupiter's Trojan asteroids

THE ASTRONOMICAL JOURNAL, 122:3485–3491, 2001 December

PLANETARY MIGRATION AND THE EFFECTS OF MEAN MOTION RESONANCES ON JUPITER'S TROJAN ASTEROIDS

T. A. MICHTCHENKO
Instituto Astronômico e Geofísico, Universidade de São Paulo, C.P. 3386, 01060-970 São Paulo, SP, Brazil; tatiana@iagusp.usp.br
C. BEAUGÉ[1]
Observatorio Astronómico, Universidad Nacional de Córdoba, Laprida 854, 5000 Córdoba, Argentina
AND
F. ROIG
Instituto Astronômico e Geofísico, Universidade de São Paulo, C.P. 3386, 01060-970 São Paulo, SP, Brazil
Received 2001 August 23; accepted 2001 September 20

ABSTRACT

We present results of several numerical simulations of fictitious Trojan asteroids under different resonant configurations of the outer planets, especially between Jupiter and Saturn. Although the present outer solar system is not locked in mean motion resonances, such commensurabilities may have been temporarily attained in the past if current theories of planetary migration are correct. By studying the evolution of Trojan-like test particles under these conditions, it is possible to obtain information related to the maximum variation of the semimajor axes of the two major Jovian planets, as well as insights on the duration of the migration itself. Results show that the 2S:1J and 5S:2J Jupiter-Saturn resonances introduce large instabilities in the Trojan region. In the case of 2S:1J, a few thousand years are sufficient to expel all particles initially in tadpole orbits. For 5S:2J, these may survive for up to 10^6 yr. The 7S:3J commensurability, on the other hand, is much less disruptive. These results seem to indicate that the observed presence of the Jovian Trojans is compatible with a planetary migration as proposed by Han & Malhotra, in which the orbital distance between Jupiter and Saturn did not vary by more about 1 AU. Larger variations of the semimajor axes seem unlikely.

Key words: celestial mechanics — minor planets, asteroids — solar system: general

1. INTRODUCTION

Almost two decades ago, Fernandéz & Ip (1984) performed a numerical simulation of the final stages of formation of the outer solar system. Starting with already formed Jupiter and Saturn, plus a rocky protoplanetary disk, they discussed the accretion of massive bodies, which could be related to the formation of Uranus and Neptune. Independently of their specific results with regard to this aim, they found an unexpected phenomenon: as a consequence of the interaction between the planetesimal disk and the planets, these latter bodies suffered significant (and secular) variations in their orbits. In particular, Jupiter showed a decrease in its orbital distance while the rest of the planets seemed to suffer an increase in their semimajor axes. Although by present-day standards their model may have been simple (e.g., the interactions between the planets themselves were neglected), this result was sufficiently important to merit further studies and confirmations using more complex numerical codes. The next decade saw a number of studies related to this subject, for example, Fernandéz & Ip (1996), Brunini & Fernandéz (1999), and Hahn & Malhotra (1999). All these works seemed to confirm the original findings of the "planetary migration" during the last stages of the formation of the outer solar system.

Although the existence of this secular variation in the orbits of the planets seemed to be generally agreed upon, the same was not true with regard to the magnitude of the migration. Hahn & Malhotra (1999) performed a series of simulations, each supposing a different mass for the protoplanetary disk ($M_{\rm disk}$). Although in all cases the direction of the migration was maintained (Jupiter decaying in orbit with the other planets increasing in orbital energy), quantitative values for Δa were a strong function of the mass of the disk. As an example, if $M_{\rm disk}$ was taken equal to 50 $M_\oplus$, the resulting planetary migration was between 0.2 AU (for Jupiter) and ≈ 7 AU (for Neptune). Obviously, higher values of $M_{\rm disk}$ yielded larger migration. Since the total mass of the protoplanetary disk is not known with any precision, it becomes difficult to specify the main parameters of the migration process, such as its magnitude and duration.

The greatest importance of planetary migration lies perhaps not in studies of planetary formation, but in its consequences for the origin and dynamics of other bodies of the solar system. Throughout many years, celestial mechanics has searched for explanations for the observed dynamical structure of main-belt asteroids and, more recently, Kuiper belt objects. All classical studies supposed that the dynamical evolution of these systems could (and should) be explained supposing that the positions of the planets (i.e., perturbing bodies) has remained unchanged since their formation. If migration really took place, then the orbits of the planets changed significantly, and this change may have had important consequences for the evolution of these small bodies. This has been the subject of numerous studies in the last few years. Applications to Kuiper belt objects (Malhotra 1993, 1995) seem to be able to explain some of the characteristics of their distribution in orbital elements. The eccentricity of Pluto, as well as its capture in the Kozai resonance, is also reproduced by applying models of migration (Malhotra 1993, 1995; Gomes 2000). It has also been proposed that the lunar late heavy bombardment could

[1] Current address: Instituto Nacional de Pesquisas Espaciais, Avenida dos Astronautas 1758, 12227-010 São José dos Campos, SP, Brazil.

have been triggered by the formation of Uranus and Neptune and the consequent migration of the Jovian planets (Levison et al. 2001). Moreover, the absence of asteroids in the Thule group, as well as their presence in the Hilda group, can also be discussed in the framework of planetary migration (Michtchenko 2001). In all cases it seems that, depending on the magnitude of the variation of the semimajor axes of the planets, many of the dynamical properties of these systems (previously unexplained) can be successfully modeled.

It has long been known that the dynamical structure of the outer planets is quasi-resonant and, thus, they lie very close to significant commensurabilities between their mean motions. Therefore, one of the main aspects of a temporal variation in the positions of the planets is the fact that they may (or should) have passed through mean motion resonances. The aim of the present paper is precisely to study the effects of temporary resonance passages, between Jupiter and Saturn, on the orbits of the Trojan asteroids. By analyzing the possible instabilities in the asteroidal motion introduced by a change in the configuration of the planets, we hope to obtain valuable information about the magnitude of the migration itself, as well as the duration of this process. A similar study was undertaken by Fleming & Hamilton (2000). However, it is important to specify that we are not going to study the effects of migration itself on the Trojans but the effects of different mean motion resonances that could have been passed (or attained) during the change in semimajor axis of the planets. This is for two reasons. First, a dynamical model in which the positions of the planets are explicitly varied does not yield information about the inner structure of the 1:1 resonance and, thus, does not allow us to understand the origins of the instabilities introduced by the resonant configurations of the planets. Second, the migration timescale is not known with any precision. Instead of adopting an ad hoc supposition, we prefer to infer maximum resonance passage times through the instabilities themselves. Moreover, it is known that the temporal variation of the orbits of the planets was not monotonic (Hahn & Malhotra 1999). The magnitude of the nonmonotonic component is not well known, and a realistic modeling of its effects is extremely difficult.

The present work is divided as follows: Section 2 presents a brief overview of the quasi-resonant structure of the outer solar system, as well as some of the dynamical characteristics of the Trojan swarm. Section 3 discusses our numerical integrations under several different configurations of the planets. Section 4 presents our main results, and finally, § 5 is reserved for the conclusions.

2. DYNAMICAL STRUCTURE OF THE OUTER SOLAR SYSTEM AND TROJAN SWARM

Although, in their current configuration, the four major outer planets (Jupiter, Saturn, Uranus, and Neptune) are not locked in mean motion resonances, there are several such commensurabilities in the immediate vicinity of the planets. These commensurabilities can be seen in Figure 1, where we have plotted a dynamical map of the region around the present position of Saturn on the (a_S, e_S)-plane of initial osculating semimajor axis and eccentricity. The dynamical map has been obtained by the spectral analysis method (SAM), described in detail in Michtchenko & Ferraz-Mello (2001). In summary, we performed a precise numerical integration of several fictitious outer solar systems, changing the initial position of Saturn. The integration was carried out using the RA15 integrator (Everhart

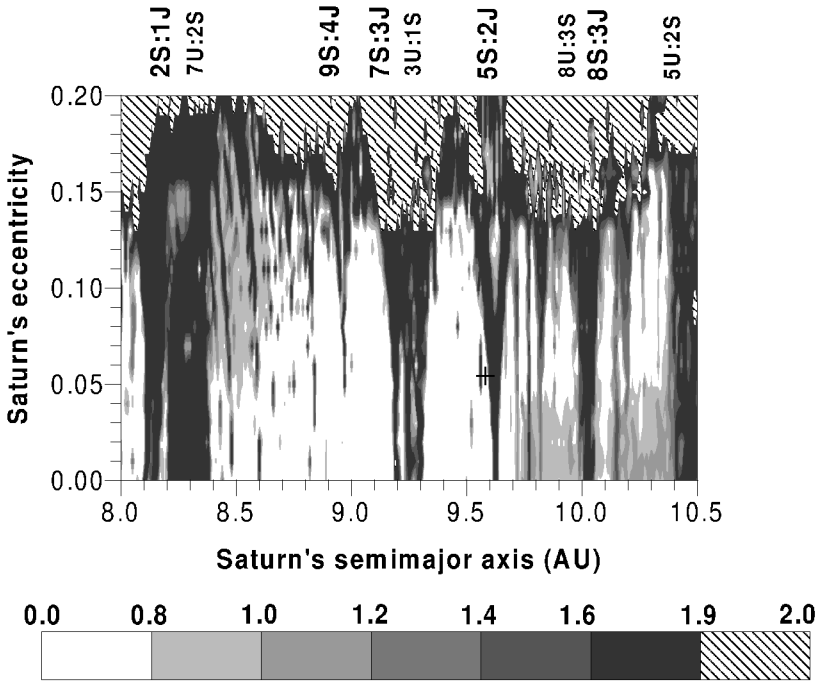

FIG. 1.—Dynamical map of the region around Saturn. The values of the spectral number N, obtained in the range from 1 to 100 over 1.5 Myr, are coded by gray levels that vary logarithmically from white ($\log N = 0$) to black ($\log N = 2$) and are plotted on the (a_S, e_S)-plane of initial osculating orbital elements. The grid of initial conditions used had 251 × 21 points, $\Delta a_S = 0.01$ AU, and $\Delta e_S = 0.01$. The lighter regions indicate regular motion, whereas the darker regions indicate chaotic motion. The domains where planetary collisions occur within 50 Myr are hatched. The actual position of Saturn is indicated by a plus sign.

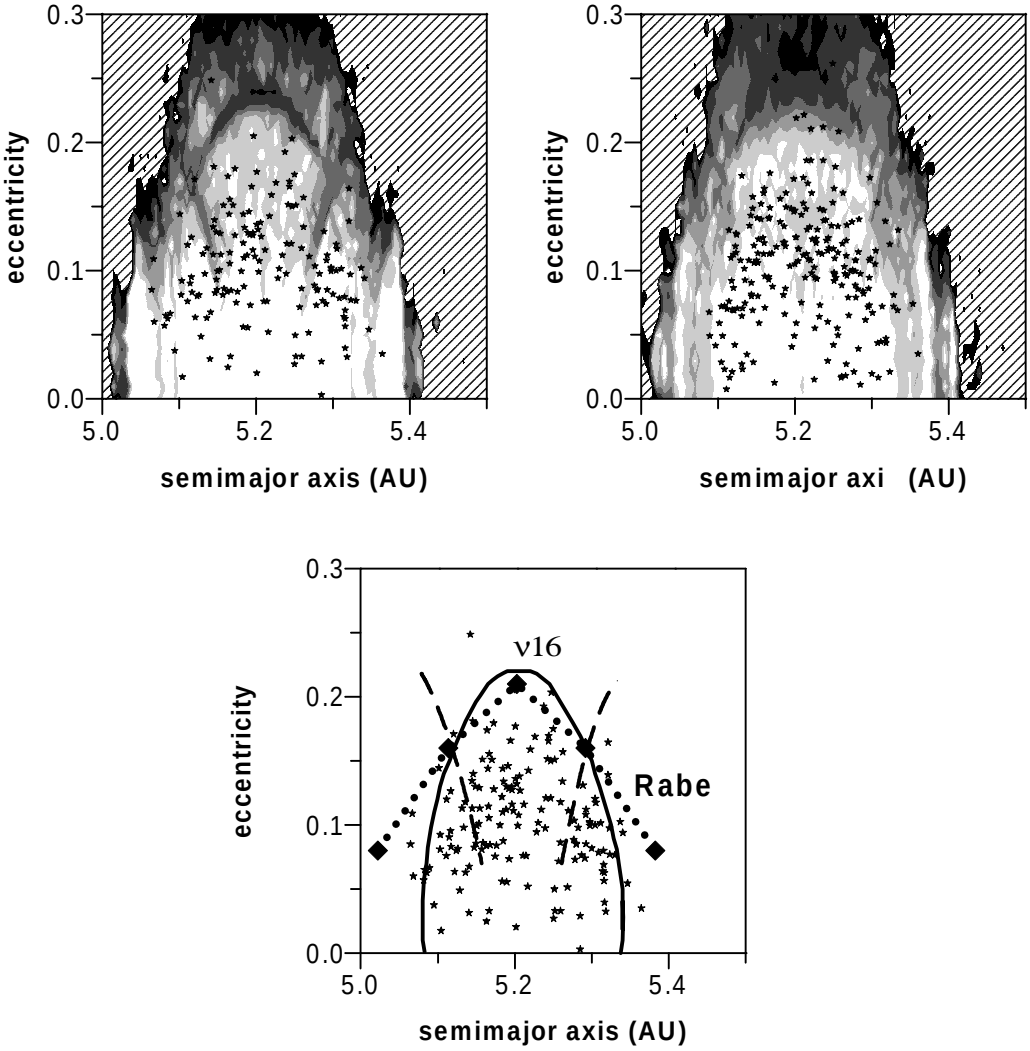

FIG. 2.—Dynamical maps of the region around the Jovian L5 Lagrange point, on the osculating (a, e)-plane. Gray-scale levels are the same as in Fig. 1. The domains where asteroidal escapes occur within 650,000 yr are hatched. The positions of the real Trojans are indicated by stars. *Top left*, plot for quasi-planar orbits; *top right*, plot for initial inclination equal to 15°; *bottom*, location of the ν_{16} secular resonance (*solid line*), Rabe's stability curve (*diamonds and dotted line*), and the superposition between the proper modes of the Jovian 1:1 resonance and the 5:2 with Saturn (*dashed lines*).

1985). The initial conditions of the fictitious Saturn were uniformly distributed in the ranges $a_S = 8.0$–10.5 AU ($\Delta a_S = 0.01$ AU) and $e_S = 0.0$–0.2 ($\Delta e_S = 0.01$). The initial positions of the other planets were chosen to be the actual ones at epoch JD 2,451,100.5. Also, the initial inclination and angular orbital elements of the fictitious Saturn were fixed at their present values. During the numerical integration, the short-term oscillations (on the order of the orbital periods) were eliminated by applying a low-pass filter to the output (see Michtchenko & Ferraz-Mello 1995). The orbital paths obtained over 1.5 Myr were Fourier-transformed, and the spectral number N was defined as the number of substantial (more than 5% of the largest peak) spectral peaks in the oscillation of Saturn's semimajor axis. Finally, the resulting values of N for each initial condition were coded using a gray-level scale that varied logarithmically from white ($\log N = 0$) to black ($\log N = 2$). They were then plotted on the (a_S, e_S)-plane of initial osculating values of the semimajor axis and eccentricity in Figure 1. Since large values of N indicate the onset of chaos, the gray-scale code is related to the degree of stochasticity of the initial conditions: white corresponds to regular orbits, while darker tones indicate increasingly chaotic motion.

The main mean motion resonances between the planets exhibit chaotic motion and appear in Figure 1 as black "stalactites" of different widths. Two-planet mean motion resonances are labeled on the top of the graph in the form $nP_j{:}mP_i$, where P denotes the planet ("J," "S," and "U" for Jupiter, Saturn, and Uranus, respectively) and n and m are the integers that appear in the critical argument of the corresponding resonance. There are also several narrow vertical bands of chaotic motion associated with three-planet resonances (see Michtchenko & Ferraz-Mello 2001). The present position of Saturn on the (a_S, e_S)-plane is marked by a plus sign. Although we note that Saturn is presently located in an apparently regular region, very close to the 5S:2J resonance with Jupiter, this may not have been true in previous times. As the planetary migration theories predict smaller values of the semimajor axis of Saturn in the past, the location of this planet should be displaced to the left in Figure 1. During migration forward to its current position, the planet may have passed through the 7S:3J and

9S:4J resonances with Jupiter and perhaps the 2S:1J Jovian commensurability. As the migration process was not uniform and monotonic (see Hahn & Malhotra 1999), it is even possible for both planets to have passed through the 5S:2J resonance. Which of these resonances were actually attained in the past obviously depends on the magnitude of the migration process. Since these passages imply temporary chaotic motion of the planets, they may have affected the orbits of smaller bodies of the solar system, whose orbits are strongly dependent on the perturbers. Possibly one of the best such candidates is the Trojan asteroids. Thus, although it may be extremely difficult to evaluate whether such passages actually occurred through analysis of the planets themselves, we may find evidence in the dynamical structure of "test particles," such as the Trojan swarm.

The Trojans are a population of several hundred observed asteroids, located in tadpole orbits around the L4 and L5 Jovian Lagrange points. Although some of them show chaotic behavior over timescales on the order of the age of the solar system (see, e.g., Milani 1993; Giorgilli & Skokos 1997), most probably have orbits sufficiently stable (Levison, Shoemaker, & Shoemaker 1997) so as to be primordial. Figure 2 shows dynamical maps of the region around the L5 point (the motion around L4 exhibits similar behavior) for two different initial asteroidal inclinations: (1) $I = 1°$ and (2) $I = 15°$. The maps were obtained by applying SAM to a 101 × 31 point grid, with $\Delta a = 0.005$ AU and $\Delta e = 0.01$. The time span of the numerical integrations of the asteroidal motion was 650,000 yr. The real Trojans (*stars*) were taken from the 2001 April version of the asteroid database of Lowell Observatory,[2] and their orbital elements were recomputed to the plane given by the conditions $\sigma = -60°$, $\varpi - \varpi_J = -60°$, and $\Omega - \Omega_J = 0°$. Here $\sigma = \lambda - \lambda_J$ is the resonant angle as a function of the mean longitudes of the asteroid (λ) and Jupiter (λ_J), ϖ and ϖ_J denote the longitudes of perihelion of each body, and Ω and Ω_J are their longitudes of node. Those objects with inclination in the range $0° < I \leq 10°$ are shown in the top left panel of Figure 2, and those with $I > 10°$ in the top right. Finally, the main dynamical structures in the vicinity of the libration region are shown in the bottom panel of Figure 2.

We note that practically all long-lived Trojans are located in the regular regions (*lighter zones*). The domains of regular motion are bounded mainly by the ν_{16} secular resonance. It is interesting to note that the location of this commensurability follows very closely Rabe's stability curve, defined as the boundary of stable tadpole orbits in the restricted three-body problem, as a function of the eccentricity (see Rabe 1965 for more details). The V-shaped chaotic domains in the central resonant region in Figure 2 (*top left*) are caused by the interactions between proper modes of the 1:1 Jovian resonance and the proper modes of the asteroidal 5:2 mean motion resonance with Saturn, which is just inside the 1:1 resonance with Jupiter. These regions are mainly found for high eccentricities and have a lower limit of about $e \approx 0.07$ (see Fig. 2, *bottom*).

The stability of Jupiter's Trojans is mostly related to the absence of significant secular resonances in the inner region around each Lagrange point. The exception is the ν_{16} resonance mentioned above, which only acts at relatively high eccentricities. The effect of the Great Inequality (the 5:2 near-commensurability between Jupiter and Saturn) inside the main libration zone is not significant (see Beaugé & Roig 2001), contrary to the case of Saturn's hypothetical Trojans (de la Barre, Kaula, & Varadi 1996). However, because of planetary migration, the location of secular resonances and planetary inequalities could be substantially shifted, and moreover, the motion of Jupiter itself could be chaotic. What would happen to the Trojan swarms in this case? This is the question we will try to answer in the following.

3. THE SIMULATIONS

In order to test this scenario, we performed a series of numerical simulations of a grid of 1581 fictitious Trojans, using several different orbital configurations for the outer planets. The simulations were carried out using RA15 in the framework of the restricted spatial N-body problem, with the Trojans as test particles, and including perturbations of four major planets. It is worth recalling that in this model the planets themselves suffer mutual perturbations.

The initial conditions for the fictitious Trojans were chosen homogeneously in a rectangular grid defined in the (a, e)-plane within the limits 5.0 AU $\leq a \leq$ 5.5 AU and $0.0 \leq e \leq 0.3$. Initial inclination was taken equal to 5° for all bodies. Angular variables were chosen such that the initial resonant angle, σ, and $\varpi - \varpi_J$ were both equal to 60° (L4 Lagrange point). The longitude of the node was taken equal to that of Jupiter. For the planets, all the orbital elements, except semimajor axes, were taken equal to their present values. The mean orbital distances of the planets were then varied in each simulation so as to place Jupiter and Saturn in different mutual mean motion resonances.

Our attention has been concentrated on three planetary resonances, namely, 2S:1J, 7S:3J, and 5S:2J. Care was taken not to introduce other commensurabilities between the remaining planets. The chosen initial values of the planetary semimajor axes were

1. $a_J = 5.30$ AU, $a_S = 8.26$ AU, $a_U = 19.276$ AU, and $a_N = 30.205$ AU, for the 2S:1J resonance;
2. $a_J = 5.28$ AU, $a_S = 9.32$ AU, $a_U = 19.0$ AU, and $a_N = 29.0$ AU, for the 7S:3J resonance;
3. $a_J = 5.203$ AU, $a_S = 9.60$ AU, $a_U = 19.276$ AU, and $a_N = 30.205$ AU, for the 5S:2J resonance.

All simulations of asteroidal motion were followed over 5 Myr. During this time span the code checked for escaped particles and was further related to their corresponding initial conditions on the (a, e)-plane. The criterion for ejection was defined in terms of the eccentricity ($e > 0.7$) and the semimajor axis ($a < 4.0$ AU or $a > 6.0$ AU). We obtained a series of maps of ejected Trojans on the (a, e)-plane for different times. It is worth recalling that the planets were not migrated during the simulation, although their orbits were allowed to vary according to their mutual gravitational effects.

4. RESULTS

We begin by studying the Jupiter-Saturn 7S:3J resonance. Since usual predictions for planetary migration assume a variation in Saturn's semimajor axis of at least 0.8 AU, a passage through this resonance seems very probable. A look at Figure 1 shows that this is, in fact, the first significant commensurability (between Jupiter's and Saturn's mean motions) located to the left of Saturn's present position. However, we must note that in Figure 1 the width of

[2] See ftp://ftp.lowell.edu/pub/elgb/astorb.html.

the chaotic region around this point is enhanced because of the overlap with the 3U:1S resonance between Saturn and Uranus. In this case, in order to avoid the interference of the 3U:1S resonance, the initial semimajor axes of Uranus and Neptune were slightly changed from their current values.

Results for the 7S:3J resonance are shown in Figure 3. Each plot is a snapshot of the escaped Trojans on the (a, e)-plane at intervals of 1 Myr, beginning at $t = 2$ Myr. Gray domains correspond to those initial conditions that are still bound to the system, while black regions indicate escaped orbits. The percentage of ejected test particles is marked at the top of each plot. After $t = 2$ Myr, all particles outside the Rabe stability region (Rabe 1965) have already escaped, as well as some high-eccentricity orbits in the vicinity of the ν_{16} secular resonance. But the central low- to moderate-eccentricity region of the resonance suffers no depletion. After $t = 3$ Myr, about 65% of the initial bodies have escaped. Instabilities are mainly due to the ν_{16} resonance (for large eccentricities) plus some evaporation close to the separatrices, which separate tadpole from horseshoe orbits. The next plot ($t = 4$ Myr) is characterized by some depletion inside the libration region itself. Nevertheless, the limits of the surviving population remain more or less constant. Finally, after $t = 5$ Myr, only about 25% of the initial population remains bounded. Their distribution is very similar to the actual Trojan bodies, although the central libration region is now affected significantly (compare with Fig. 2). We may therefore conclude that the present dynamical structure of the Trojans seems to be consistent with a planetary migration that crossed the 7S:3J Jupiter-Saturn resonance, even if this passage lasted as long as 4 million years.

Figure 4 shows the results for the 2S:1J commensurability. According to Figure 1, this resonance is located at about 1.4 AU from the present location of Saturn, and it will have been crossed only if we assume about twice the planetary migration suggested by Hahn & Malhotra (1999). We can see from our simulation that the effect of this resonance on the Trojan swarms is much more destructive. After only 5000 yr, over 85% of the test particles have been ejected. This number increases to 100% after less than 10,000 yr of integration time. Although a much larger instability should be expected in this case with respect to the 7S:3J resonance, its sheer magnitude was surprising. This result seems to indicate that either planetary migration never reached this point or, maybe, the passage through the 2S:1J commensurability lasted only a few hundred years. However, this latter hypothesis seems rather unlikely. Recent simulations by Beaugé, Roig, & Nesvorný (2001) show that if the initial position of Saturn is chosen at 8 AU, and the value of the planetesimal disk ($M_{\rm disk}$) chosen so as to induce a migration to its present orbit, then the transition time inside the 2S:1J resonance should be about 5×10^5 yr.

Finally, Figure 5 presents results for the 5S:2J Jupiter-Saturn resonance. According to Figure 1, this resonance is located to the right of Saturn's present location, but as we mentioned in § 1, a nonmonotonic variation of the semimajor axes of these planets could have temporarily put them in this commensurability. From our simulations, we

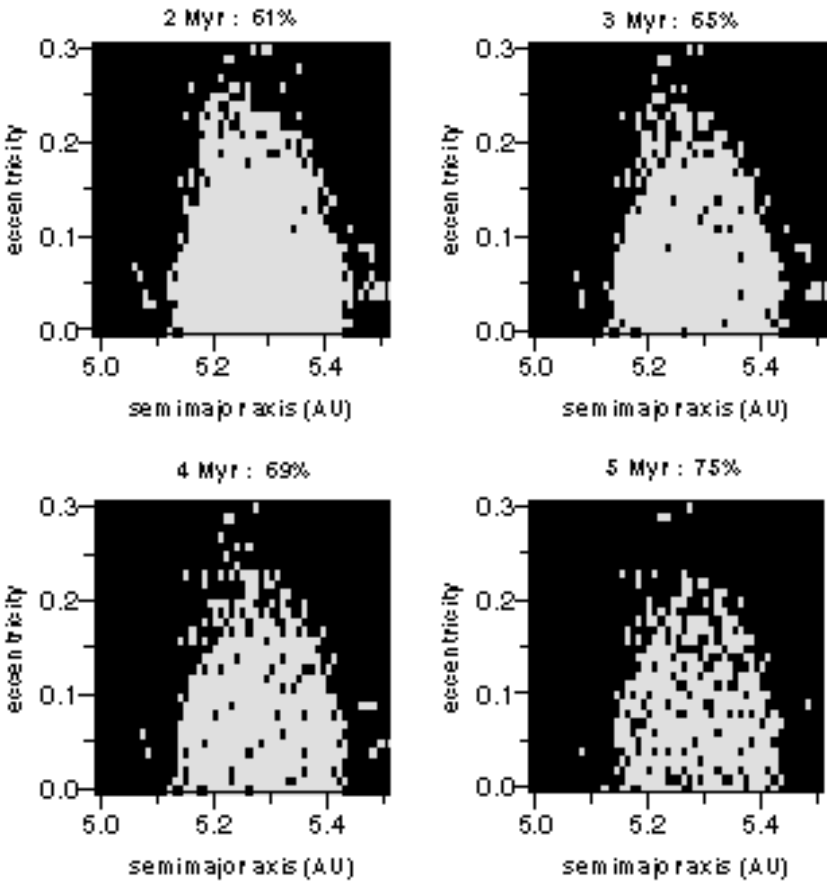

FIG. 3.—The (a, e)-planes of initial conditions for the test particles, at four different intermediate times during the integration, when Jupiter and Saturn are in the 7S:3J mean motion resonance. Gray regions correspond to survivors, whereas black regions correspond to escaped bodies. The percentage of test particles ejected from the region is marked at the top of each plot.

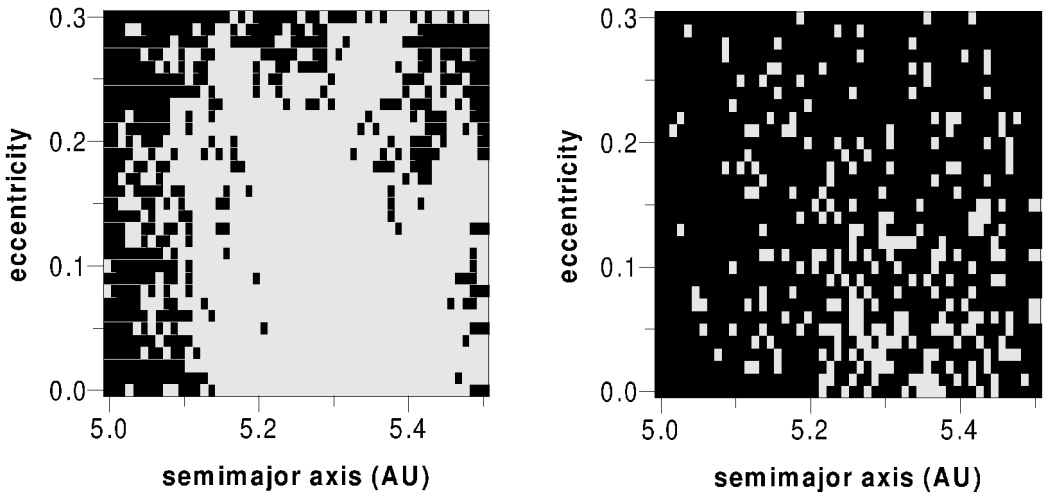

FIG. 4.—Results for Jupiter and Saturn in the 2S:1J mean motion resonance. Color code is the same as in Fig. 3. Integration times are 2000 yr (*left*) and 5000 yr (*right*).

can see that the instability introduced by this resonance is quite large. Even though it is not so destructive as the 2S:1J resonance, we see that after 1.5 Myr almost all the test particles are depleted. Moreover, even after only 500,000 yr the depletion is already significant. Thus, if a passage of the planets through this commensurability effectively happened, it probably lasted no more than a few hundred thousand years.

Although all our simulations provide evidence of instabilities generated inside the Jovian Lagrange points, we have still not discussed their causes. Two different explanations are possible. First, the new configurations of the planets may shift (and perhaps intensify the effects of) the secular resonances inside the libration zone. Second, the chaotic motion of Jupiter related to the planetary commensurability may, in turn, generate large-scale stochasticity in the Trojan region. This may occur directly through a chaotic change in the location of the Lagrange points themselves, or through large-scale sweeping of the inner resonances. Both these effects are, in truth, mixed and unfortunately cannot be analyzed separately in a numerical simulation. Nevertheless, we can perform indirect calculations.

In order to test the first hypothesis, we determined the position of ν_{16} and Rabe's stability curve for each of the different planetary configurations to see whether they showed any significant displacement. This was done using the same spectral analysis method employed for the construction of the bottom panel of Figure 2. Results show that the value of the fundamental frequency of Saturn's node g_6 shows only small changes, and the position (and size) of the ν_{16} resonance remains practically unchanged. The same holds for Rabe's curve. This seems to imply that the instabilities observed in our simulations are probably not related to changes in the structure of secular resonances.

A second possibility is an enhancement of the interactions between the proper modes of the 1:1 Jovian resonance and mean motion commensurabilities with Saturn. Since both planets are now placed in resonance lock, it is reasonable to expect an increase in the importance of these effects. An example can be seen in Figure 5 (*left*), where, after only 500,000 yr, the V-shaped chaotic domain due to the 5:2 resonance with Saturn is already much more pronounced than in Figure 2 (*top left*). Nevertheless, even though this hypothesis may very well explain the ejection of particles in the immediate vicinity of such internal reso-

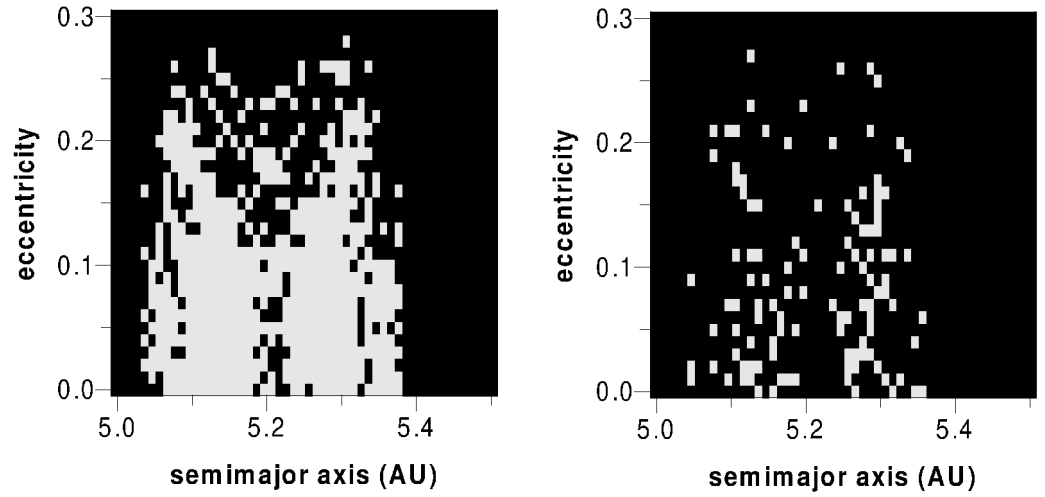

FIG. 5.—Results for Jupiter and Saturn in the 5S:2J mean motion resonance. Color code is the same as in Fig. 3. Integration times are 500,000 yr (*left*) and 1.5 Myr (*right*).

nances, the region outside them should still be populated. Unfortunately, this is not the case. A look at the right panel of Figure 5 shows that after only 1.5 Myr the whole tadpole region is practically depleted.

It therefore seems necessary to assume that the chaotic motion of the planets themselves makes a significant contribution to the instabilities of the Trojan orbits. This could be either directly, through large-amplitude variations in the orbit of Jupiter, or indirectly, as a result of large-scale sweeping of the internal resonances with Saturn. Once again, both effects are related and it seems difficult to identify which is more important. Perhaps additional and more detailed simulations could provide us an answer and confirm this mechanism.

5. CONCLUSIONS

We have presented a series of numerical simulations of the evolution of test particles inside the Jovian 1:1 resonance, in the case where Jupiter and Saturn are artificially placed in mutual mean motion resonant configurations. The results show that in certain cases, the passage of Jupiter and Saturn through those commensurabilities located close to their present positions can introduce very significant instabilities in the orbits of the real Trojans. The origin of these instabilities would be mainly due to the chaotic behavior of Jupiter itself.

We have studied three different resonances, namely, 2S:1J, 7S:3J, and 5S:2J. In each case, we analyzed the instabilities induced on the test particles and their escape times, and we have been able to deduce the approximate upper bounds for the magnitude of the planetary migration and to provide some insight on the timescale of this process.

The extremely large chaoticity generated by the 2S:1J resonance on the test bodies seems to indicate that the planets never crossed this point in the past. Thus, it appears unlikely that the primordial relative positions of the Jupiter-Saturn pair differed from present values by more than 1 AU. Larger values of planetary migration are incompatible with the observed presence of asteroids in the L4 and L5 Jovian Lagrange points, if we assume that Trojans are primordial objects.

The 5S:2J resonance also introduces significant instabilities in the Trojan region on timescales on the order of 1 Myr. Thus, if the planets ever temporarily reached this point, the passage could not have lasted much more than 1 Myr. This result may be important for two reasons. First, it can be thought of as an independent confirmation of the direction of the planetary migration, i.e., the primordial distance between Jupiter and Saturn could not have been larger than the present one, but only smaller. Second, it also places upper bounds for the nonmonotonic behavior of the variation of the semimajor axes. This limit can be thought of either in terms of size or in terms of duration. Thus, if Jupiter and Saturn were, even temporarily, more distant in the past, this configuration could not have been kept for more than 1 Myr.

At last, the 7S:3J resonance does not seem to generate any significant instabilities over timescales on the order of 4 Myr. From this result we can find no evidence to say that such a configuration may not have been attained in the past. We may conclude that the present population of the Trojan asteroids is compatible with a planetary migration in which (1) the variation of the distance between Jupiter and Saturn was at most 1.4 AU, (2) the passage through the 7S:3J resonance lasted at most 4 Myr, and (3) any nonmonotonic component of the migration was either very small or lasted less than about a million years.

This work has been supported by the Brazilian research foundations (FAPESP projects 00/07084-0 and 97/05806-9 and CNPq project 300946/96-1) and the Computation Center of the University of São Paulo (LCCA). The authors are grateful to Professor S. Ferraz-Mello for a critical reading of the manuscript.

REFERENCES

Beaugé, C., & Roig, F. 2001, Icarus, in press
Beaugé, C., Roig, F., & Nesvorný, D. 2001, in preparation
Brunini, A., & Fernandéz, J. A. 1999, Planet. Space Sci., 47, 591
de la Barre, C. M., Kaula, W. M., & Varadi, F. 1996, Icarus, 121, 88
Everhart, E. 1985, in IAU Colloq. 83, Dynamics of Comets, ed. A. Carusi & G. B. Valsecchi (Dordrecht: Reidel), 185
Fernandéz, J. A., & Ip, W.-H. 1984, Icarus, 58, 109
———. 1996, Planet. Space Sci., 44, 431
Fleming, H. J., & Hamilton, D. P. 2000, Icarus, 148, 479
Giorgilli, A., & Skokos, C. 1997, A&A, 317, 254
Gomes, R. S. 2000, AJ, 120, 2695
Hahn, J. M., & Malhotra, R. 1999, AJ, 117, 3041
Levison, H. F., Dones, L., Chapman, C. R., Stern, S. A., Duncan, M. J., & Zahnle, K. 2001, Icarus, 151, 286
Levison, H. F., Shoemaker, E. M., & Shoemaker, C. S. 1997, Nature, 385, 42
Malhotra, R. 1993, Nature, 365, 819
———. 1995, AJ, 110, 420
Michtchenko, T. A. 2001, in preparation
Michtchenko, T. A., & Ferraz-Mello, S. 1995, A&A, 303, 945
———. 2001, AJ, 122, 474
Milani, A. 1993, Celest. Mech. Dyn. Astron., 57, 59
Rabe, E. 1965, AJ, 70, 687

5. Conclusões gerais

Nesta tese estudamos a evolução dinâmica a longo prazo de três populações de corpos menores em ressonâncias de movimentos médios: (i) o grupo de Zhongguo, na ressonância 2/1 com Júpiter, (ii) o grupo dos Plutinos, na ressonância 2/3 com Netuno, e (iii) o grupo dos Troianos, na ressonância 1/1 com Júpiter. O estudo foi desenvolvido, principalmente, através de simulações numéricas do problema de N corpos, levando em conta as perturbações gravitacionais dos planetas Jovianos.

No caso da ressonância 2/1, achamos que o grupo de Zhongguo (por volta de 30 asteróides) é estável ao longo da idade do Sistema Solar, mas a sua distribuição de tamanhos indica que sua origem poderia estar vinculada a um fenômeno recente de fragmentação dentro da prórpia ressonância. Não encontramos evidências de que estes asteróides tenham sido injetados desde fora da ressonância 2/1, exceto no caso de captura em ressonância induzida pela migração planetária. Por outro lado, existe uma população de asteróides ressonantes instáveis que pode ser re-alimentada continuamente com objetos de fora da ressonância através de diversos mecanismos dinâmicos, como a difusão devida às ressonâncias fracas na vizinhança da ressonância 2/1 e o efeito Yarkovsky.

Quanto a ressonância 2/3 com Netuno, ela constitui um dos maiores reservatórios dos cometas de curto período no cinturão de Kuiper. Nossas estimativas indicam que deveria existir uma população de aproximadamente 600 milhões de cometas, dos quais só conseguimos observar atualmente por volta 30 objetos. Os objetos observados ficam

distribuídos dentro dos limites de estabilidade da ressonância, mas as suas amplitudes de libração particularmente grandes ($\sim 80°$) evidenciam a influência do efeito gravitacional do planeta Plutão.

Finalmente, construímos um modelo semi-analítico para estudar a dinâmica da ressonância 1/1 e determinar elementos próprios dos Troianos de Júpiter. Com nossos resultados identificamos as famílias de asteróides e achamos que existe uma diferença significativa entre os Troianos de L_4, onde existem duas famílias bem definidas, e os Troianos de L_5, onde não se observam famílias. A estabilidade dos Troianos foi analisada no âmbito da migração planetária, encontrando-se que a existência da população observada atualmente é compatível com a idéia clássica de migração, onde Júpiter e Saturno atravessam a ressonância mútua 7/3, mas não as ressonâncias 2/1 e 5/2.

Nossos resultados certamente irão contribuir para uma melhor compreensão dos problemas que estudamos, mas ainda estão longe de fornecer uma solução definitiva aos mesmos. Muito pelo contrário, eles abrem uma série de novas perguntas a serem respondidas e desafios a serem estudados, entre os quais podemos destacar:

- Fazer observações espectroscópicas do grupo de Zhongguo, para tentar confirmar a idéia de uma origen colisional recente destes asteróides. Estas observações poderiam ser complementadas com estudos mais detalhados sobre as probabilidades de colisão dos asteróides na ressonância 2/1, e com simulações precisas da fragmentação de um objeto ressonante e a posterior evolução dinâmica dos fragmentos.

- Analisar a estabilidade a longo prazo do grupo de Zhongguo sob o efeito da migração planetária ou de pequenas mudanças na Grande Desigualdade, para ver se isto pode justificar efetivamente a ausência de asteróides na região central da ressonância 2/1.

- Utilizar modelos realísticos de fragmentação de asteróides, baseados, por exemplo, em códigos hidrodinâmicos, para avaliar com precisão a possibilidade de injetar fragmentos na ressonância 2/1 como conseqüência da formação da família de Themis.

- Estudar as conseqüências do fenômeno de formação da binária Plutão-Caronte, no âmbito do regime de co-rotação entre os Plutinos e Plutão, tentando determinar

se poderia existir uma população relevante de Troianos de Plutão.

- Explicar a existência de famílias de asteróides nos Troianos de Júpiter em torno de L_4, e sua aussência em torno de L_5. Este problema poderia ser abordado de diversas formas, desde a procura por eventuais diferenças na estabilidade a longo prazo dos dois pontos Lagrangeanos, ou por diferenças na evolução colisional dos dois grupos, até pela existência de "bias" observacional entre as duas populações.

- Tentar identificar as famílias de asteróides Troianos de Júpiter através de observações espectroscópicas, da mesma forma que foi feito com as famílias do cinturão principal (Florczak et al 1998, 1999).

- Analisar a estabilidade dos Troianos e outros grupos de asteróides através de modelos de migração planetária mais realísticos que os utilizados até o momento, que levem em conta, principalmente, o fato da migração não ter sido um processo "contínuo e linear". Estes modelos poderiam ser utilizados também para analisar com mais detalhe a probabilidade de captura em ressonância, e as eventuais conseqüências da migração planetária sobre os cinturão primordial dos asteróides (ex., Liou e Malhotra 1997; Gomes 1997) e o cinturão de Kuiper (Malhotra 1995).

Ainda temos pela frente muito caminho por andar e, afortunadamente, ele esta semeado de inúmeros problemas em aberto.

Bibliografia

Beaugé, C., e Roig, F.: 2001. *Icarus* **153**, no prelo.

Benz, W., e Asphaug, E.: 1999. *Icarus* **142**, 5–20.

Bien, R., e Schubart, J.: 1987. *Astron. Astrophys.* **175**, 292–298.

Duncan, M.J., Levison, H.F., e Budd, S.M.: 1995. *Astron. J.* **110**, 3073–3081.

Duncan, M.J., Quinn, T., e Tremaine, S.: 1988. *Astrophys. J. Lett.* **328**, L69–L73.

Fernández, J.A.: 1980. *MNRAS* **192**, 481–491.

Fernández, J.A., e Ip, W.-H.: 1984 *Icarus* **58**, 109–120.

Ferraz-Mello, S.: 1994. *Astron. J.* **108**, 2330–2337.

Ferraz-Mello, S., e Klafke, J.C.: 1991. Em *Predictability, Stability and Chaos in N-body Dynamical Systems*, A.E. Roy (Ed.), Plenum Press, pp. 177–184.

Ferraz-Mello, S., e Sato, M.: 1989. *Astron. Astrophys.* **225**, 541–547.

Ferraz-Mello, S., Michtchenko, T.A., e Roig, F.: 1998. *Astron. J.* **116**, 1491–1500.

Ferraz-Mello, S., Michtchenko, T.A., Nesvorný, D., Roig, F., e Simula, A.: 1998. *Planet. Space Sci.* **46**, 1425–1432.

Florczak, M., Barucci, M.A., Doressoundiram, A., Lazzaro, D., Angeli, C., e Dotto, E.: 1998. *Icarus* **133**, 233–246.

Florczak, M., Lazzaro, D., Mothé-Diniz, T., Angeli, C., e Betzler, A.: 1999. *Astron. Astrophys. Suppl. Ser.* **134**, 463–471.

Gomes, R.: 1997. *Astron. J.* **114**, 396–401.

Gomes, R.: 1998. *Astron. J.* **116**, 2590–2597.

Gomes, R.: 2000. *Astron. J.* **120**, 2695–2707.

Greenberg, R., e Franklin, F.: 1976. *MNRAS* **173**, 1–8.

Hahn, J.M., e Malhotra, R.: 1999. *Astron. J.* **117**, 3041–3053.

Henrard, J., Milani, A., Murray, C.D., e Lemaitre, A.: 1983. *Celest. Mech.* **38**, 335–344.

Henrard, J.: 1990. *Cel. Mech. Dyn. Astr.* **49**, 43–67.

Holman, M., e Wisdom, J.: 1993. *Astron. J.* **105**, 1987–1999.

Holman, M., e Murray, N.: 1996. *Astron. J.* **112**, 1278–1293.

Hori, G.: 1966. *PASJ* **18**, 287–296.

Jewitt, D., e Luu, J.: 1993. *Nature* **362**, 730–732.

Kirkwood, D.: 1867. Meteoric astronomy: a treatise on shooting stars, fireballs and aerolites. J.B. Lippincott, Philadelphia.

Klafke, J.C., Ferraz-Mello, S., e Michtchenko, T.A.: 1992. Em *Chaos, Resonance and Collective Dynamical Phenomena in the Solar System*, S. Ferraz-Mello (Ed.), Kluwer, Dordrecht, pp. 153–158.

Knežević, Z., Milani, A., Farinella, P., Froeschlé, Ch., e Froeschlé, C.: 1991. *Icarus* **93**, 316–330.

Levison, H.F., e Duncan, M.J.: 1993. *Astrophys. J. Lett.* **406**, L35–L38.

Levison, H.F, e Duncan, M.J.: 1994. *Icarus* **108**, 18–36.

Levison, H.F., e Stern, S.A.: 1995. *Icarus* **116**, 315–339.

Levison, H.F., Shoemaker, E.M., e Shoemaker, C.S.: 1997. *Nature* **385**, 42–44.

Liou, J.C., e Malhotra, R.: 1997. *Science* **275**, 375–377.

Malhotra, R.: 1995, *Astron. J.* **110**, 420–429.

Malhotra, R.: 1996. *Astron. J.* **111**, 504–516.

Marzari, F., e Scholl, H.: 1998. *Icarus* **131**, 41–51.

Marzari, F., Farinella, P., Davis, D.R., Scholl, H., e Campo Bagatin, A.: 1997. *Icarus* **125**, 39–49.

Michtchenko, T.A., e Ferraz-Mello, S.: 1995. *Astron. Astrophys.* **303**, 945–963.

Michtchenko, T.A., e Ferraz-Mello, S.: 1996. *Astron. Astrophys.* **310**, 1021–1035.

Michtchenko, T.A., e Ferraz-Mello, S.: 1997. *Plan. Space Sci.* **45**, 1587–1593.

Milani, A.: 1993. *Cel. Mech. Dyn. Astr.* **57**, 59–94.

Moons, M., e Morbidelli, A.: 1995. *Icarus* **114**, 33–50.

Moons, M., Morbidelli, A., e Migliorini, F.: 1998. *Icarus* **135**, 458–468.

Morais, M.H.: 2001. *Astron. Astrophys.* **369**, 677–689.

Morbidelli, A.: 1996. *Astron. J.* **111**, 2453–2461.

Morbidelli, A.: 1997. *Icarus* **127**, 1–12.

Morbidelli, A., e Moons, M.: 1993. *Icarus* **103**, 99–108.

Morbidelli, A., e Nesvorný, D.: 1999. *Icarus* **139**, 295–308.

Morbidelli, A., Thomas, F., e Moons, M.: 1995. *Icarus* **118**, 322–340.

Morbidelli, A., Zappalà, V., Moons, M., Cellino, A., e Gonczi, R.: 1995. *Icarus* **118**, 132–154.

Murray, C.D.: 1994. *Icarus* **112**, 465–484.

Murray, N., e Holman, M.: 1997. *Astron. J.* **114**, 1246–1259.

Nesvorný, D., e Ferraz-Mello, S.: 1997a. *Astron. Astrophys.* **320**, 672–680.

Nesvorný, D., e Ferraz-Mello, S.: 1997b. *Icarus* **130**, 247–258.

Nesvorný, D., e Morbidelli, A.: 1998. *Astron. J.* **116**, 3029–3037.

Petit, J.M., e Farinella, P.: 1993. *Cel. Mech. Dyn. Astr.* **57**, 1–28.

Roig, F., e Ferraz-Mello, S.: 1999. *Planet. Space Sci.* **47**, 653–664.

Roig, F., Simula, A., Ferraz-Mello, S., e Tsuchida, M.: 1998. *Astron. Astrophys.* **329**, 339–349.

Rubincam, D.P.: 1995. *J. Geophys. Res.* **100**, 1585–1594.

Sidlichovský, M., e Melendo, B.: 1986. *Bull. Astr. Inst. Czech.* **37**, 65–80.

Vokrouhlický, D., Milani, A., e Chesley, S.: 2000. *Icarus* **148**, 118–138.

Wisdom, J.: 1982. *Astron. J.* **87**, 577–593.

Wisdom, J.: 1987. *Icarus* **72**, 241–275.

Zappalà, V., Cellino, A., Farinella, P., e Knežević, Z.: 1990. *Astron. J.* **100**, 2030–2046.